

Reply to the Reviewer 1:

I thank the authors for addressing my comments. The paper has been improved, although language editing is necessary. The remaining surprising result is that the coupled model, which suffers from a 4 W m⁻² radiative imbalance, manages to produce a non-drifting preindustrial control simulation. It seems likely that the coupled model does not conserve energy or that some energy flows are not diagnosed properly. I suggest to mention in the conclusion these imbalance and the potential issues that they hint at.

We thank all the reviewer suggestions. An English proofreading was hired (editing certificate is attached here). The requested discussion about the radiative imbalance at the top-of-atmosphere is added in the Conclusion section.

Reply to the Reviewer 2

Review of "Assessing the performance of climate change simulation results from BESM-OA2.5 in comparison to a CMIP5 model ensemble" by V.B. Capistrano et al. (revised manuscript)

Overall assessment and recommendation

I regret to conclude that this paper has not been sufficiently improved by the revision process to be acceptable. While I appreciate that the authors have tried to bring the characteristics of BESM-OA2.5 more in focus of their presentation (rather than discussing the general performance of CMIP5 models), the results is still a clumsy and partly dis-organized concatenation of results and result comparisons that do not lead to a clear assessment of the suitability of BESM for specific purposes. New text often has been insufficiently harmonized with the previous text, making reading through the manuscript still an extremely arduous task.

As I stated in my original review, my impression is that BESM is a reasonable model that could be useful for specific applications at least. Hence, I am reluctant to reject this paper once and for all. The authors should be allowed to make one more attempt to create a straightforward paper with a coherent message. To this end (as I have proposed before) the focus of future use of BESM should be made clear, considering the merits and shortcomings of this model. The authors should intensify their attempts to interlink the evidence arising from individual parameter evaluation. This already has been tried in a number of cases, but it too often results in circular reasoning, not approaching the roots of characteristic BESM features. Finally, I emphasize that just executing through my list of technical and language suggestions alone will not do! The author team apparently does not include an English native speaker, hence assistance in producing a proper English text ought to be given by either the editorial office or from some other consultant. Otherwise, I fear that I will be reluctant to read through this paper once again.

We thank all the reviewer suggestions. The manuscript was rewrite to make each the paragraph message clearer. Furthermore, as requested, an English proofreading was hired (editing certificate is attached here).

General remarks

- 1) Section 2.1 still contains elements of a comparison between BESM-OA2.5 and BESM-OA2.3 (e.g., p. 3, l.32) though a dedicated section (2.2) is supposed to cover such differences.

Reply: This comparison was removed and a new discussion was added in the section 2.2.

- 2) It is on occasions still hard to reproduce what has actually been done and why (e.g., p. 6, l.25).

Reply: Please see the section about Language and Technical Remarks below.

- 3) No reason is given on p. 8, 2nd paragraph, why only 11 rather than 15 CMIP5 models are included here. Or are sometimes 11, sometime 15, models used, as could be read out of p. 8, l. 6?

Reply: Andrews et al. (2012) used 15 CMIP5 models and we used 26, which means that we added 11 models. We reorganized the paragraph.

- 4) Occasionally, I still miss a comment on the specific performance of BESM, even if it's well consistent with the CMIP5 ensemble (e.g. Figure 3).

Reply: The requested information were added.

- 5) Page 9, 1st paragraph: This has been reformulated, but is now even more confusing than before. Please reconsider, what is the intended message here, with focus on BESM. Then stick to specific reasoning to underpin that message.

Reply: The paragraph was rewrite to make the main message clear.

- 6) Page 9, 2nd paragraph: Here, too, the line of reasoning remains badly organized: What is the message: Does BESM simulate a stronger Arctic amplification than the CMIP ensemble (suggested by the more negative Planck feedback)? This could simply explain more snow/ice melting. Evidently the lapse rate feedback in BESM is exceptionally positive at Arctic latitudes, pointing at a enhanced vertical gradient in the temperature response. Can this be discussed in the context of the Veiga et al. paper (atmospheric temperature response)?

Reply: The paragraph was rewrite to make the main message clear.

- 7) The last paragraph of section 4.2, with much newly introduced text, is very hard to understand both concerning the weak use of English language and a confusing inherent logic. I have read through this paragraph three times, but then

gave up, being unable to reconcile the statements in the text with what the figures display.

Reply: The paragraph was rewrite to make the main message clear.

8) Scatter Diagrams in Figures 8 and 9: Do you conclude anything from the apparent correlation between precipitation in piControl and abrupt4xCO₂ on one side, and missing correlation for respective surface temperature levels on the other side? Does this have implications for the BESM model performance.

Reply: BESM results were included and linked previous discussions.

9) In the last paragraph of the conclusions an outlook to what is planned with BESM-OA2.5 (future research focus) is still lacking. However, this would be the logical outcome of the assessment of its merits and shortcomings, which I assume is what the present paper has been written for.

Language and Technical Remarks

p. 1, l. 7 (Abstract): “ ... the CMIP5 ensemble mean value ... ”

Reply: The climate feedback responses were estimated for 25 CMIP5 models individually and for BESM, no just for the CMIP5 ensemble. This strategy as adopted in order to visualize where BESM in comparison to a distribution of climate response.

p. 1, l. 8 (Abstract): “ ... BESM simulation show zonally average feedbacks, estimated from radiative kernels, that lie within the ensemble standard deviation ... ”

Reply: Done.

p. 1, l. 11 (Abstract): “... BESM also features a strong positive ...”

Reply: Done.

p. 1, l. 12 (Abstract): As this sentence mentions a merit of BESM, while the preceding sentence comments on a disagreement with CMIP, “moreover” makes quite an unlucky connection. By the way, “consistent” with what?

Reply: “Moreover” was changed to “However”. The BESM results are consistent with the CMIP5 ensemble mean. Changes were done to clarify this point.

p. 2, l. 7: “... results in a temperature rise ...”

Reply: Done.

p. 3, l. 7: “... models, also discussing peculiarities in the BESM climate response.”

Reply: Done.

p. 3, l. 16: "... same as used by Veiga ..."

Reply: Done.

p. 3, l. 17: "... model, with its dynamical core being based on ..."

Reply: Done.

p. 3, l. 22: "... of physical parameterizations between BAM (as used in this paper) and BAM NWP ..."

Reply: Done.

p. 3, l. 24: "... 28 layers, unevenly spaced, in the ..."

Reply: Done.

p. 3, l. 29: "... is able to capture ..."

Reply: Done.

p. 3, l. 30: "... with a double ITCZ ..."

Reply: Done.

p. 3, l. 31: "improvement", despite of the "substantial biases" addressed in the preceding sentence?

Reply: This sentence was adapted to "Comparison to previous version" section as requested in the general considerations.

p. 3, l. 33: "... decadal climate variability patterns." This is meant, isn't it?

Reply: Yes. It is correct now.

p. 4, l. 4: I understand that AMOC is a circulation structure rather than a parameter. So, what "value" are you referring to? If required, please give an absolute or relative difference of the parameter you have in mind.

Reply: The AMOC strength simulated by the model in the piControl is around 14 Sv (for 1000 years). The AMOC strength observed by the RAPID project is roughly 17 Sv (McCarthy et al. 2015).

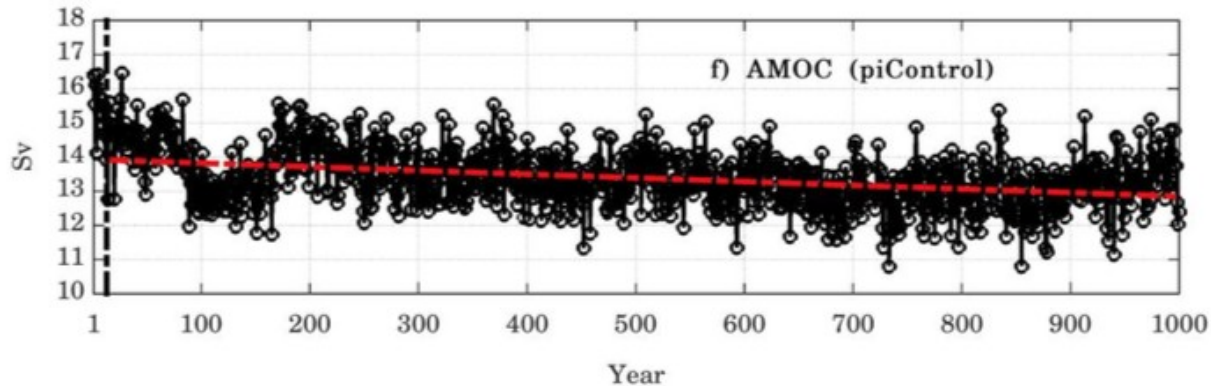


Figure - Maximum AMOC simulated by the piControl from the beginning of the simulation up to 1000 years. The red dash-dot lines shows the linear trend.

p. 4, l. 9: "... are determined, which are important ...". Anyway, the content of this sentence to me resembles what is given below (p. 4, l. 14), with the sentences in between (starting with "The total energy balance ...") causing an awkward logical break.

Reply: In order to avoid this apparent logical break, the sentence "which are important in the coupling between atmosphere and ocean" was removed. The section emphasizes the main differences between BESM versions, that are in the atmospheric model parametrization, specially in the way the diagnostic surface layer variables are calculated. The general differences in the atmospheric model are discussed first, and just after this is introduced more details about surface layer variables (where was found a repetition about the importance of these variables for the ocean-atmosphere coupling).

p. 4, l 19: This sentence again repeats what is given in p. 4, l. 9 ...

Reply: Please, see the immediately above answer.

p. 5, l. 6: "... which means a spin-up of 150 years." Does this mean that the 150 yrs of abrupt4xCO₂ are regarded as a spin-up here (due to their non-equilibrium character)? Or are 150 yrs of abrupt4xCO₂ swapped as a spin-up, and *another* 150 yrs evaluated as some kind of quasi-equilibrium? Please, clarify.

Reply: The piControl spin-up of 150 years means that the piControl run for 150 years before the analysed period. Therefore, after the 150 yr run, two new simulations of 150 yr are started: 1) the piControl continuation run; 2) the Abrupt4XCO₂ run. New informations are added to manuscript text.

p. 5, l. 6: "... commonly employed ... for climate change assessment"; please, be careful to distinguish between "climate change assessment" and "climate sensitivity assessment"! In my view, "climate change" in the CMIP context is rather assessed

through historical simulations and future scenario simulations.

Reply: "...climate change assessment" is changed to "...climate sensitivity assessment" in the new version.

p. 5, l. 12: In this paragraph the "forth and back" jumping in addressing the merits of the regression and kernel method is somewhat confusing but could be easily avoided.

Reply: The "forth and back" jumping was avoided in this version.

p. 5, l 27, 28: There's still something wrong with the sentences here. Suggestion: "As G can be approximated by backward regression towards $\Delta T_{as}=0$, ECS can be estimated as $ECS=-G/\lambda$."

Reply: The alteration proposed was done. The intention with the original sentence was emphasize the computation economy that the regression method allows, avoiding a simulation in a order of millenia. The following sentence was removed: "For this method the ECS can be estimated as $ECS=-G/\lambda$ in a shorter simulation (typically of 150 year) without reach the thermodynamical equilibrium.".

p. 5, l 30: "... it is common to divide the result derived from 4xCO₂ simulations by 2 (Andrews ..."

Reply: Done.

p. 6, l. 9: "... is used next, in order to partition the ...", as "next to" is confusing. By the way, "separate" or "split" may be preferred to "partition".

Reply: Done. It was used "decompose" instead of "partition"

p. 6, l. 14: "integrally" -> "fully" (or "necessarily")

Reply: Done. "integrally" was replaced by "necessarily".

p. 6, l. 16: "This, however, assumes that ..."

Done.

p. 6, equation 3: T_{as} is the near surface temperature (p. 5), but what is then T_s ? I tried to clarify this by looking into Vial et al. (2013), without success. Please, be precise in citing, or explaining what you have done, and why.

Reply: T_s means surface temperature whereas T_{as} means near-surface atmospheric temperature. In order to avoid misunderstandings, besides Vial et al. (2013) was cited Soden and Held (2006, page 3356), which has a good compatibility with the variables presented in the equation 3 of our work.

p. 6, l. 25: Confusing: As q is in the data base, why should it be approximated based on the assumption of constant relative humidity? To my knowledge, this is not common in feedback analysis. Is it possible that you are misinterpreting the cited references here?

Reply: The assumption of constant relative humidity is associated with how the water vapor kernel is obtained. For water vapor kernel, it is computed the specific humidity change corresponding to a 1-K increase (holding relative humidity constant). Please see Soden et al. (2008) page 3509 and Shell et al. (2008) page 2271.

Additional information about the necessity of this assumption was included in consonance with what was requested in the general comments.

p. 7, l. 5: "... changes are not accounted ..."

Reply: Done.

p. 7, equation 5: It is not immediately obvious, what the indices "a" and "k" mean.

Reply: The index "k" means the change in ΔCRE due to the noncloud feedbacks, while the index "a" means the ΔCRE adjusted (to obtain the cloud feedback). Additional information was provided to this new manuscript version.

p. 8, l. 4: "... were assessed as it was performed ..."; I do not understand this sentence. Are the data not from the ESGF data base (p. 5, l. 10) ??

Reply: The sentence is to inform the reader that we used the same method (analysis, assessment or evaluation) realized by Andrews et al. (2012). This is not supposed to be link with a mention to ESGF.

p. 8, l. 6: "... e inmcm4 ", did you intend "... and inmcm4"?

Reply: Done.

p. 8, l. 13: witch -> which

Reply: Done.

p. 8, l. 29: Please, explain how Figure 4 is related to Figure 3. Is it simply an average over the latitudinal profile of Fig. 3? Your discussion of the Planck feedback is casting doubts concerning this: If it's constant by about $-4 \text{ Wm}^{-2}\text{K}^{-1}$ (l.29) with mostly negative deviations at polar latitudes, how can this result in a global mean of $-3.6 \text{ Wm}^{-2}\text{K}^{-1}$ (l. 26)? Please, cross-check the numbers.

Reply: a) The Figure 3 shows the global mean for the climate feedbacks, where is possible note the models dispersion. The Figure 4 shows the same feedbacks (and the Planck feedback) but for the zonal average.

b) The ensemble Planck feedback is about $-3.39 \text{ W/m}^{-2}\text{K}^{-1}$ at the Equator (as well as in the Tropics). It has values below -10 near North Pole, however, we can not forget that the global mean is calculated considering the areal weight for each latitude, which is smaller for polar zones. Therefore, the global mean features a value around $-3.6 \text{ W/m}^{-2}\text{K}^{-1}$

p. 8, l. 32: "stronger vertically homogeneous warming". This is a strange reasoning, as the Planck feedback is essentially the surface warming, constantly extrapolated upward through the depth of the troposphere. Can the message of this sentence be reconciled with Figure 8?

Reply: a) We totally agree with the comments. By definition the Planck feedback assumes that the temperature change is vertically uniform throughout the troposphere with respect to surface (Soden et al. ,2008, page 3515). This is in the Eq. (4) of the manuscript:

$$\lambda_p = \left(K_{T_s} \frac{dT_s}{dT_{as}} + K_T \frac{dT_s}{dT_{as}} \right)$$

This also is in accordance with what is stated by Jonko et al. (2013): "The Planck feedback is the response of longwave (LW) TOA flux to a perturbation in surface temperature that is applied to each vertical layer of the troposphere."

On the other hand, the lapse-rate feedback is related to the radiative response to changing the vertical temperature structure.

Therefore, it was added more information regarding the relation of the Planck feedback and surface temperature.

b) It add more information mentioned the link between Figure 8 and results from figures 3 and 4.

p. 9, l. 20: The partly revised text in this paragraph (see also major comments) contains some sensible elements, but is also moving in circles, explaining stronger sea-ice melting with stronger surface warming and vice versa. More re-organisation of the text is necessary.

Reply: Modifications were performed as requested in the major remarks.

p. 9, l. 22: "Those negative values ...", it is unclear which values are addressed.

Reply: It is about negative Planck feedback. Such paragraph was reorganized.

p. 9, l. 30: "The highest positive values ...", I would expect that backscattering increases if ice turns into water, driving the shortwave cloud feedback to *more negative* values. However, your later discussion (Figure 7, see also below) seems to suggest that the longwave cloud feedback is the dominant component.

Reply: This whole paragraph was rewrite. Since the ice has a greater albedo than water, when occurs sea-ice melting the albedo decreases, consequently, the outgoing shortwave radiation at the TOA also decreases. Two aspects are highlighted in the high latitudes for BESM cloud feedback: a weak increase in total cloud cover, which contributes to a negative SW cloud feedback (Figure 6a-b); and a low-level clouds upward shifting that is responsible for a gain of LW energy, which is related to sea-ice melting and indirect linked to albedo feedback cloud mask (Figure 6 c-d).

p. 9, l. 31: I feel that the following text (until "... outlier for the cloud feedbacks.") is mainly repetitive.

Reply: I was rewrite.

p. 10, l. 4: " λ_a , λ_{ac} ", are you referring to an analytical framework that is given in Cess et al. (1989)? Otherwise the reader is rather left in the dark here.

Reply: They are in the Equation (5). " λ_a , λ_{ac} " are the albedo feedback and the albedo feedback for clear-sky, respectively. More information is added to clarify the discussion.

p. 11, l. 4: "models with ... apparently do not show ..."; please also replace "present" by "show" on many occasions thereafter.

Reply: Done.

p. 11, l. 24: "...quadrupling of atmospheric CO₂ with the piControl pre-industrial CO₂ concentrations ...": meaning what? The two first sentences of this paragraph appear to transport the same statement.

Reply: Real meaning is: "...quadrupling of atmospheric CO₂ with respect to the piControl pre-industrial CO₂ concentrations ...". It was changed for the new version.

p. 11, l. 28: "... precipitation increase is not governed ..."

Reply: Done.

p. 11, l. 31: Does this have in any way implications for the use of these somewhat "outlying" models?

Reply: The fact that a model is an outlier in one feature does not invalidate that model in others features. For example, HadGEM2 is widely recognized for having a good representation of precipitation in many parts of the globe; however, it is on the list indicated in the manuscript that models do not have a linear fit between global warming and precipitation change. Such behaviour may be due to chosen tuning in physical parameterization.

p. 12, l. 13: "...regions with the strongest increase of westerly winds at all levels indicate a southward jet displacement ..."

Reply: Done.

p. 12, l.18: Is "omega" something different from "vertical velocity"? Anyway, "omega" isn't self-explaining, so please adjust the text.

Reply: Omega is related to vertical velocity, but is not the same variable. Omega is Dp/Dt (isobaric coordinates), while vertical velocity is $w=Dz/Dt$ (height coordinates). For hydrostatic approximation $Dp/Dz = -\rho g$ with ρ constant, $\Omega = -\rho g w$. In order to clarify the sentence we changed "vertical velocity" to "omega vertical motion".

p. 12, l. 31: "... radiative code transference ...", do you mean "performance"? Is there any indication of that particular feature for BESM's radiative transfer model?

Reply: It is related to BESM's radiative transfer model. The correction was done.

p. 12, l. 31: "... rapid adjustments ..."; the rapid adjustment process is included in the CMIP5 model results as well, per construction. You apparently did not calculate the rapid adjustments for BESM, but do you have any indications that there might be a systematic bias with respect to CMIP (see Smith et al., 2018).

Reply: We did not integrated the BESM (atmosphere-only: BAM) model with climatological SST and ice cover doubling CO₂ in order to evaluate the rapid adjustments. However, we think that this could be done a future study.

p. 13, l. 4: "Two regions indicate enhanced inter-model standard deviation for Planck, lapse-rate and albedo feedback"; also in the rest of this paragraph the use of English language is very weak, making the meaning nearly incomprehensible for me.

Reply: The entire paragraph has been rewritten and a third party English proofreading service has been performed.

References (only if not already cited in the paper):

Smith, C.J. et al., 2018: Understanding rapid adjustments to diverse forcing agents, Geoph. Res. Lett. 45, 12023-12031.

References cited in the responses:

Andrews, T., Gregory, J. M., Webb, M. J., and Taylor, K. E.: Forcing, feedbacks and climate sensitivity in CMIP5 coupled atmosphere-ocean climate models, *Geophysical Research Letters*, 39, n/a–n/a, <https://doi.org/10.1029/2012GL051607>, 2012.

McCarthy, G.D.; Smeed, D.A.; Johns, W.E.; Frajka-Williams, E.; Moat, B.I.; Rayner, Darren.; Baringer, M.O.; Meinen, C.S.; Collins, J.; Bryden, H.L. (2015): Measuring the Atlantic Meridional Overturning Circulation at 26°N, *Progress in Oceanography*, 130: 91–111. doi:10.1016/j.pocean.2014.10.006

Jonko, A. K., Shell, K. M., Sanderson, B. M., and Danabasoglu, G.: Climate Feedbacks in CCSM3 under Changing CO₂ Forcing. Part II: Variation of Climate Feedbacks and Sensitivity with Forcing, *Journal of Climate*, 26, 2784–2795, <https://doi.org/10.1175/JCLI-D-12-00479.1>, 2013.

Shell, K. M., Kiehl, J. T., and Shields, C. a.: Using the radiative kernel technique to calculate climate feedbacks in NCAR's Community Atmospheric Model, *Journal of Climate*, 21, 2269–2282, <https://doi.org/10.1175/2007JCLI2044.1>, 2008.

Soden, B. and Held, I.: An Assessment of Climate Feedbacks in Coupled Ocean – Atmosphere Models, *Journal of Climate*, 19, 3354–3360, <https://doi.org/10.1175/JCLI9028.1>, 2006.

Soden, B. J., Held, I. M., Colman, R., Shell, K. M., Kiehl, J. T., and Shields, C. A.: Quantifying Climate Feedbacks Using Radiative Kernels, *Journal of Climate*, 21, 3504–3520, <https://doi.org/10.1175/2007JCLI2110.1>, 2008.

EDITORIAL CERTIFICATE

This document certifies that the designated manuscript was edited for correct English language, punctuation, grammar, spelling, and overall style by a qualified and experienced native English-speaking editor.

Authors

Vinicio Buscioli Capistrano, Paulo Nobre, Sandro Veiga, Renata Tedeschi, Josiane Silva, Marcus Bottino, Manoel Baptista da Silva Junior, Otacílio Leandro Menezes Neto, Silvio Nilo Figueroa, José Paulo Bonatti, Paulo Yoshio Kubota, Julio Pablo Reyes Fernandez, Emanuel Giarolla, Jessica Vial, and Carlos A. Nobre

Manuscript Title

Assessing the performance of climate change simulation results from BESM-OA2.5 compared with a CMIP5 model ensemble

Date Issued

04 January 2020

Certification Key

BES2644-5308-6690-6891-4317A

To verify this certificate, please visit www.bioplicityediting.org/certification and enter the complete Certification Key. Neither the authors' original intended meaning, nor the research contents were altered during the editing process; however, the authors can accept or reject the editorial changes as they wish. To verify that the final submitted version was edited by Bioplicity Editing Service, the Certification Key will provide access to the last-edited version. If you have any questions or concerns about this document, please contact info@bioplicityediting.org.

Assessing the performance of climate change simulation results from BESM-OA2.5 ~~in comparison to compared with~~ a CMIP5 model ensemble

Vinicius Buscioli Capistrano^{1,2}, Paulo Nobre¹, Sandro Veiga¹, Renata Tedeschi¹, Josiane Silva¹, Marcus Bottino¹, Manoel Baptista da Silva Junior¹, Otacílio Leandro Menezes Neto¹, Silvio Nilo Figueroa¹, José Paulo Bonatti¹, Paulo Yoshio Kubota¹, Julio Pablo Reyes Fernandez¹, Emanuel Giarolla¹, Jessica Vial³, and Carlos A. Nobre⁴

¹Center for Weather Forecast and Climate Studies/National Institute for Space Research (CPTEC/INPE), Cachoeira Paulista – São Paulo, Brazil

²Amazonas State University (UEA), Manaus – Amazonas, Brazil.

³Laboratoire de Météorologie Dynamique/Centre National de la Recherche Scientifique (LMD/CNRS), Paris, France

⁴National Center for Monitoring and Early Warning of Natural Disasters (CEMADEN), São José dos Campos – São Paulo, Brazil

Correspondence: Vinicius Buscioli Capistrano, Amazonas State University, 1200 Darcy Vargas Ave., 69050-020, Manaus – Amazonas, Brazil (vcapistrano@uea.edu.br)

Abstract. The main features of climate change patterns, as simulated by the coupled ocean-atmosphere version 2.5 of the Brazilian Earth System Model (~~BESM-OA2.5~~) ~~are contrasted~~ ~~BESM~~, ~~are compared~~ with those of ~~other~~ 25 ~~other~~ CMIP5 models, focusing on temperature, precipitation and atmospheric circulation. The climate sensitivity to quadrupling ~~the~~ atmospheric CO₂ concentration ~~is investigated from two techniques: the~~ ~~was investigated via two methods:~~ linear regression (Gregory et al.,

5 2004) and ~~Radiative Kernel~~ (Soden and Held, 2006; Soden et al., 2008) ~~methods~~ ~~radiative kernel~~ (Soden and Held, 2006; Soden et al., 2008). Radiative kernels from both NCAR and GFDL ~~are used in order~~ ~~were used~~ to decompose the climate feedback responses of ~~the~~ CMIP5 models and ~~BESM-OA2.5~~ ~~BESM~~ into different processes. ~~Applying~~ ~~By applying~~ the linear regression method for equilibrium climate sensitivity (ECS) estimation, we ~~obtain a value for BESM~~ obtained a BESM value close to the ensemble mean value. ~~The~~ ~~This~~ study reveals that ~~BESM has shown zonally averaged feedbacks estimated from Radiative Kernel~~ ~~the~~ 10 ~~BESM simulation yields zonally average feedbacks, as estimated from radiative kernels, that lie~~ within the ensemble standard deviation of ~~the other CMIP5 models~~. ~~The exceptions are~~ ~~. Exceptions were~~ found in the high-latitudes of the Northern Hemisphere and ~~over~~ the ocean near ~~Antarctic~~ ~~Antarctica~~, where BESM ~~shows~~ ~~showed~~ values for lapse-rate, humidity feedbacks and albedo ~~marginally out~~ ~~that were marginally outside~~ of the standard deviation of ~~the values from the~~ CMIP5 multi-model ensemble. For those areas, BESM also ~~presented an~~ ~~featured a~~ strong positive cloud feedback ~~being a outlier comparatively~~ 15 ~~to~~ ~~that appeared as an outlier compared with~~ all analyzed models. ~~Moreover, BESM shows~~ ~~However, BESM showed~~ physically consistent changes in the ~~pattern of~~ temperature, precipitation and atmospheric circulation ~~patterns relative to the CMIP5 ensemble mean~~.

1 Introduction

The effects of increased atmospheric CO₂ ~~concentration~~ concentrations on the climate system ~~has~~ have been studied over the last 120 years (Arrhenius, 1896; Callendar, 1938; Plass, 1956; Kaplan, 1960; Manabe and Wetherald, 1967, 1975; Manabe and Stouffer, 1980; IPCC, 2007, 2013; Pincus et al., 2016; Good et al., 2016, and many others). The ~~human induced increase of human-induced increase in~~ atmospheric greenhouse gas (GHG) concentrations, sometimes given as the CO₂-equivalent concentration, contributes to a radiation imbalance at the ~~Top-Of-Atmosphere~~ top-of-atmosphere (TOA), ~~causing that causes~~ less outgoing radiation to leave the Earth ~~System~~ system. The trapping of infrared radiation results in a temperature rise at the lower levels of the troposphere, as well as an increase in ocean ~~heating~~ heat content. In addition, the increased GHG concentration can ~~act as a trigger for trigger~~ climate feedback processes that ~~will~~ either amplify or damp the initial radiative perturbation (Cubasch and Cess, 1990). Earth system models (~~ESM~~ ESMs) are the most advanced tools available for analyzing the coupled climate system (atmosphere, ocean, land, and ice) physical processes and their interactions, although ~~they even these models~~ still exhibit important uncertainties in their projections of climate change (IPCC, 2013).

The equilibrium global-mean surface temperature change induced by doubling the CO₂ concentration in the atmosphere, referred to as the ~~Equilibrium Climate Sensitivity~~ equilibrium climate sensitivity (ECS), remains a centrally important measure of a model's climate response to CO₂ forcing. In the fifth Intergovernmental Panel on Climate Change (IPCC) assessment report (AR5), climate model ~~estimates of the ECS range from 2~~ ECS estimates range from 2.0 K to 4.5 K. For more than 40 years, this inter-model spread has been considered one of the most critical uncertainties for the evaluation of future climate ~~changes~~ change (IPCC, 2013). This inter-model dispersion arises principally from differences in how the climate models simulate climate feedback processes. Among them, ~~the~~ cloud feedback constitutes the largest source of ~~spread for variation in~~ the climate sensitivity estimates (Cess et al., 1989, 1990; Dufresne and Bony, 2008; Vial et al., 2013; Caldwell et al., 2016).

Beyond the ECS, the response of ~~precipitation~~ the precipitation patterns to anthropogenic GHG emissions is a topic of great interest in climate science, given ~~the potential consequences~~ their potential effects on both societies and ecosystems. Changes in precipitation can generally be decomposed into two processes: a thermodynamic component due to increased moisture and no circulation change, and a dynamic component due to circulation change ~~and with~~ no moisture change (Bony et al., 2006; Seager et al., 2010). The thermodynamic component gives rise to the well-known 'wet-gets-wetter' and 'dry-gets-drier' ~~pattern of precipitation changes~~ patterns of precipitation change first described by Held and Soden (2006), which ~~is associated with are associated with the~~ Clausius-Clapeyron relation (i.e., a ~~temperature-dependent exponential increase in the~~ saturation-specific humidity ~~increase exponentially with temperature~~) (Marvel and Bonfils, 2013). ~~As to the dynamic component~~ The dynamic component, which is associated with circulation change, ~~it~~ sometimes yields strong deviations from the thermodynamic pattern of precipitation, and ~~this component~~ is known to dominate the uncertainty in estimates of total precipitation due to uncertainties in the regional circulation change (Xie et al., 2015).

The recent development of the Brazilian Earth System Model, ocean-atmosphere coupled version 2.5 (BESM-OA2.5) is an evolution of BESM-OA2.3 first presented by Nobre et al. (2013). The authors scrutinized the BESM-OA2.3 model behavior for decadal climate variability and climate change using extended runs with ensemble members totaling over 2000 years of model simulations. El Niño/Southern Oscillation (ENSO) interannual variability over the equatorial Pacific and the inter-hemispheric 5 gradient mode over the tropical Atlantic on decadal time scale are reproduced by BESM-OA2.3. Veiga et al. (2019a) showed that BESM-OA2.5 is able to simulate the general mean present-day climate state, as well as to reproduce the main climate variability, particularly over the Atlantic.

Here ~~In this study~~, we assess the main features of climate change patterns as simulated by ~~the Brazilian Earth System Model, ocean-atmosphere coupled version 2.5~~ (BESM-OA2.5), with a focus on temperature (climate sensitivity and feedbacks), precipitation and atmospheric circulation. The recent development of the BESM-OA2.5 ~~is~~has been a coordinated effort ~~of~~at the National Institute for Space Research (INPE) in Brazil ~~in order intended~~ to advance the understanding of the causes of ~~the~~ global and regional climate changes and their ~~impaets~~ effects on the socioeconomic sector. We evaluate how ~~BESM's~~ simulated climate change ~~compares with the BESM-simulated climate change prediction compares with those from~~ Coupled Model Intercomparison Project phase 5 (CMIP5) models, ~~discussing peculiarity of BESM also discussing peculiarities in the~~ 10 ~~BESM-OA2.5~~ climate response. ~~The~~ This paper is structured as follows: section 2 presents the description of the new features of ~~BESM2-OA2~~BESM-OA2.5, section 3 presents the methodology, ~~the results are presented in section 4~~ ~~presents the results~~, and section 5 presents the summary and conclusions. 15

2 Model Description

2.1 BESM-OA2.5

The coupled model BESM-OA2.5 ~~model~~ is the result of coupling the Center for Weather Forecast and Climate Studies (CPTEC/INPE) Brazilian Atmospheric Model [BAM (Figueroa et al., 2016)] and the Geophysical Fluid Dynamics Laboratory (GFDL) Modular Ocean Model version 4p1 (Griffies et al., 2004) via the Flexible Modular System (FMS) ~~(also from GFDL)~~. The dynamical core and physical processes of the atmospheric component of BESM-OA2.5 ~~is the same that used by Veiga et al. (2019a)~~ are the same as those used by Veiga et al. (2019b). BAM is a hydrostatic model, ~~which with~~ its dynamical core ~~is~~ based on the spectral transform method ~~which employs the~~, which employs global spherical harmonic basis functions. The Eulerian ~~Advection~~ advection scheme option is used in this study but with ~~a~~ two-time-level semi-Lagrangian scheme for the transport of moisture and microphysics prognostic variables, which are carried out completely ~~on within~~ the model grid space. Simplified fast physical parametrizations are used here ~~due to computationally efficiency requirements for long integrations in comparison that used in to increase the computational efficiency of long integrations, thus resulting in a decreased computational demand compared with that required by~~ the operational Numerical Weather Prediction (NWP) model. The A summary of the main differences in ~~physical processes between BAM~~ the physical parameterizations between BAM (as used in this paper~~and~~) and the BAM NWP operational ~~is listed~~ model is provided in Table 1. The dynamical equations in BAM are discretized following a spectral transform with horizontal resolution truncated at triangular wavenumber 62 (~~approximately~~

an equivalent grid size of approximately 1.875°) and 28 layers unevenly spaced in the vertical sigma coordinate with the top level at ~~around~~ approximately 2.73 hPa. The oceanic component uses a tripolar grid at a horizontal resolution of 1° in longitude, and in the latitudinal direction the grid spacing is $1/4^\circ$ between 10°S - 10°N , decreasing uniformly to 1° at 45° and to 2° at 90° in both hemispheres. The ocean grid has 50 vertical levels with a 10-m resolution in the upper 220 m, decreasing gradually to 5 about approximately 370 m at deeper levels.

Veiga et al. (2019a) Veiga et al. (2019b) showed that BESM-OA2.5 ~~is able to simulate~~ can capture the general mean climate state. ~~However, however,~~ substantial biases ~~appear at~~ appeared in the simulation associated with a double ITCZ over the Pacific and Atlantic Oceans and regional biases in the precipitation over the Amazon and Indian regions. ~~It is worth noting that BESM-OA2.5 shows improvement in ITCZ representation in comparison with the previous version (Nobre et al., 2013)~~ 10 BESM-OA2.5 ~~also is capable to~~ can also reproduce the most important large-scale interannual and decadal climate ~~variabilities~~ variability patterns. The Atlantic Meridional Mode (AMM) (Nobre and Shukla, 1996) is well simulated by the model in ~~term of the terms of its~~ spatial pattern and temporal variability, whereas this mode is poorly represented in most CMIP5 models (IPCC, 2013; Liu et al., 2013; Richter et al., 2014; Amaya et al., 2017). The maximum strength of the Atlantic Meridional Overturning Circulation (AMOC) represented by BESM-OA2.5 ~~has a mean circulation which is similar~~ is 14 Sv, which is lower than the value 15 observed by the RAPID project [17 Sv; McCarthy et al. (2015)] but in the range of the observed root-mean-square variability, and this value is comparable to the ensemble AMOC simulated by the CMIP5 models, ~~but slightly lower than the averaged value based on observation~~. Moreover, the spatial structure structures of both the North Atlantic Oscilation Oscillation (NAO) and the Pacific Decadal Oscillation (PDO) variability is well captured (Veiga et al., 2019a) are well captured (Veiga et al., 2019b).

2.2 Comparison to a previous version

20 The recently developed BESM-OA2.5 is an evolution of BESM-OA2.3, which was presented by Nobre et al. (2013). The main differences between BESM-OA2.5 and the previous version (BESM-OA2.3described in Nobre et al. (2013) are) lie in the atmospheric model and how some surface layer variables are estimated, ~~which are important in the coupling between atmosphere and ocean~~. The total energy balance at the TOA is better represented in BESM-OA2.5 than in BESM-OA2.3, which results in an improvement that reduced ~~to around the mean global bias to approximately~~ -4 W m^{-2} ~~the mean global bias of,~~ 25 compared with -20 W m^{-2} presented by for the latter. It should be noted that BESM-OA2.5 has a new set of parameterizations, mainly ~~regarding a better related to an improved~~ related to an improved microphysical processes representation. For instance, the ~~previous model precipitation~~ precipitation in the previous model was parameterized only in terms of the ~~large scale~~ large-scale condensation. Moreover, BESM-OA2.5 underwent improvements in the representation of ~~the~~ wind, humidity and temperature in the surface layer, with the use of the similarity functions formulation method presented by Jiménez et al. (2012). Based on Monin-Obukhov 30 theory, the wind (u_{10m}), humidity (q_{2m}) and temperature (θ_{2m}) are estimated from the values of the first atmospheric model level and the surface, as described in Eq. (24), (25) and (26) of Jiménez et al. (2012). Furthermore, the similarity functions ψ_m and ψ_h depend on the stability regimes (Businger et al., 1971). For BESM-OA2.5, those regimes are associated with stable ($\zeta/L > 0$) and unstable ($\zeta/L \leq 0$) conditions (Arya, 1988). ~~These~~ These diagnostic variables are important for BESM because they are used in the ocean-atmosphere coupling strategy.

5 ~~One-year-long~~ Both versions reproduce the main climate variability, particularly over the Atlantic, as the AMOC and the AMM, but simulate a weak El Niño/Southern Oscillation (ENSO) interannual variability over the equatorial Pacific (Nobre et al., 2013; Veiga et al., 2019b). Concerning the general mean present-day climate state, BESM-OA2.5 shows improvements in reproducing the Intertropical Convergence Zone (ITCZ), and it reduces both the global precipitation root-mean-square error (RMSE) and the SST RMSE compared with those modeled by BESM-OA2.3.

10 One-year-long global simulations and ~~6-hourly outputs were done~~ 6-hourly outputs were performed with BAM configured with surface layer schemes based on Arya (1988) and Jiménez et al. (2012), here called BAM-Arya (the original scheme) and BAM-Jimenez (the new scheme), respectively. The normalized ~~root mean square error (RMSE)~~ RMSE was computed with respect to the reanalysis NCEP-DOE (National Centers for Environmental Prediction – Department of Energy) version 2 (Kanamitsu et al., 2002). The normalized RMSE of the wind at 10 m ~~and the~~ temperature and humidity at 2 m for the two surface layer schemes were investigated. Consistent improvements of BAM-Jimenez relative to BAM-Arya were noted in all ~~the~~ three variables over the oceanic regions. The normalized RMSE analysis over the continents presented less consistent results, with improved BAM-Jimenez representation of both winds and temperature, but ~~degraded with an inferior~~ representation of the humidity field (figures not shown).

15 3 Methodology

3.1 ~~Experiments~~ Experimental design

For ~~the purpose of~~ this study, climate simulations ~~are~~ ~~were~~ performed using BESM-OA2.5 (hereinafter BESM) for the pi-
Control (pre-industrial control scenario, run for 300 years with atmospheric CO₂ concentration invariant at 274 ppmv) and
abrupt4xCO₂ (run for 150 years after the abrupt quadrupling of atmospheric CO₂ at year ~~150~~ ~~151~~ of the piControl simulation)
20 scenarios, ~~which means a spin-up of~~; ~~therefore, both experiments were run in parallel for~~ 150 years. These two scenarios
~~that~~ are commonly employed in CMIP5 studies for climate ~~change~~ sensitivity assessment (Taylor et al., 2012; Eyring et al.,
25 2016). Climate change is evaluated ~~from~~ as the difference between the abrupt4xCO₂ and piControl experiments. In addition,
BESM's results ~~are~~ ~~were~~ compared with a selection of 25 CMIP5 models listed in Table 2. All models, including BESM, ~~are~~
~~were~~ interpolated at 2.5° x 2.5° longitude/latitude horizontal resolution. All CMIP5 ~~models~~ model data are available ~~in~~ from
the Earth System Grid Federation (ESGF).

3.2 ~~Estimates of climate~~ Climate change sensitivity estimates

Here we estimate the climate feedback using two different ~~techniques~~ methods: regression (Gregory et al., 2004) and ~~Radiative Kernel~~ (Soden et al., 2004, 2008) ~~method~~ radiative kernel (Soden et al., 2004, 2008). The Gregory method ~~has a more straightforward computation, however~~ is more straightforward computationally; however, it returns only a global-mean value. Moreover, the
30 ECS can be estimated with this method. On the other hand, it is possible to obtain the seasonal feedback for every lat-lon

point with Radiative Kernel method, besides the radiative kernel method; furthermore, the feedback can be decomposed into different processes. Moreover, with the linear regression method, it is possible to estimate the ECS.

3.2.1 Linear forcing-feedback regression analysis

The regression method to compute for computing the thermal response to radiative forcing is was applied for 26 CMIP5 models, including BESM. The method consists of the linear regression between the annual change (considering abrupt4xCO₂ minus piControl) of the global-mean near-surface temperature (ΔT_{as}) and the net radiation change (ΔR) at the TOA.

If G is the radiative forcing imposed on the climate system (here, associated with an abrupt increase in atmospheric CO₂ concentration) and ΔR is the resulting radiative imbalance in the global-mean net radiative budget at the TOA, then at any time, the response of the climate system to this radiative imbalance responds corresponds to the radiative forcing according to the following equation:

$$\Delta R = \lambda \Delta \bar{T}_{as} + G \quad (1)$$

where λ (< 0) is the climate feedback parameter and $\Delta \bar{T}_{as}$ is the global-mean near-surface temperature change. In a sufficiently long simulation (coupled atmosphere-ocean models take millennia), when the climate system reaches a new equilibrium (when $\Delta R = 0$. As G can be approximated via backward regression towards $\Delta \bar{T}_{as} = 0$). For this method the ECS can be estimated as ECS = $-G/\lambda$ in a shorter simulation (typically of 150 year) without reach the thermodynamical equilibrium ECS = $-G/\lambda$. As the ECS is the theoretical equilibrium temperature for doubling CO₂CO₂, in a quadrupling of CO₂ it is necessary to divide its result CO₂ it is common to divide the result derived from 4xCO₂ simulations by 2 (Andrews et al., 2012).

By using this linear forcing-response framework, we can estimate climate sensitivity, radiative forcing, and feedback parameter following the method proposed by Gregory et al. (2004). The values of λ (slope) and G (y-intercept) are estimated through the ordinary least square via the ordinary least-square regression of the global-annual-mean of ΔR against $\Delta \bar{T}_{as}$ in under all-sky conditions. Using the same linear technique, we decompose the feedback parameter into shortwave (SW) and longwave (LW) radiation components, and we extract the clear-sky clear-sky radiative flux components from the BESM and CMIP data-bases in order databases to estimate the cloud radiative forcing or cloud radiative effect (ΔCRE) defined as the difference between the all-sky and clear-sky feedback parameters (Andrews et al., 2012). Estimates of G , λ , ΔCRE , and ECS for all models are presented in the next section.

3.2.2 Climate feedbacks (Radiative Kernel radiative kernel)

The radiative kernel technique [as in Soden and Held (2006), Soden et al. (2008), Vial et al. (2013)] is used next to partition to separate the feedback parameter λ into contributions from the temperature response (λ_T), water vapor (λ_{lnq}), surface albedo (λ_a), and cloud (λ_c) feedbacks plus a residual term (Re(Vial et al., 2013), and) (Vial et al., 2013) as expressed in Eq. (2).

$$\lambda = \lambda_T + \lambda_{lnq} + \lambda_a + \lambda_c + Re \quad (2)$$

It is worth noting that in the regression method the radiative feedback is consistent with the actual radiative transfer scheme used in the climate model, while in the radiative kernel the feedback is not integrally consistent. In fact, the kernel is obtained from another climate model that is not among the models analyzed. Model intercomparison is easily achieved using this method as the same kernel can be applied to all models (Soden and Held, 2006; Soden et al., 2008, 2018). This however assumes that 5 the kernel is independent of models and climate states and that uncertainties in the radiative transfer code used to compute them are small compared to the models' climate responses (Soden et al., 2008). We used both GFDL (Soden et al., 2008) and National Center for Atmospheric Research (NCAR) (Shell et al., 2008) radiative kernels to estimate climate feedbacks. Such radiative kernels consist of the impact in the radiative balance in the TOA via arbitrary increases in the atmospheric temperature, albedo 10 and specific humidity. For the temperature kernel, 1-K is added for all model levels (including the surface). In the albedo kernel, the albedo value is increased by 0.01 (1%). Finally, for the water vapor kernel, the specific humidity is increased by a value equivalent to a 1-K atmosphere temperature increase, with the relative humidity remaining constant. Furthermore, we used the $\ln(q)$ instead of q , considering the quasi proportionality of the absorption of radiation by water vapor to $\ln(q)$.

Following Soden and Held (2006) and Vial et al. (2013), we decompose the total feedback parameter (λ) into contributions from λ_T , $\lambda_{\ln q}$, λ_a , and λ_c as:

$$\begin{aligned} \lambda &= \sum_x \lambda_x + \text{Re} = \sum_x \frac{\partial R}{\partial x} \frac{dx}{d\bar{T}_{as}} + \text{Re} = \sum_x K_x \frac{dx}{d\bar{T}_{as}} + \text{Re} \\ \lambda &= \left(K_{T_s} \frac{dT_s}{d\bar{T}_{as}} + K_T \frac{dT}{d\bar{T}_{as}} \right) + \left(K_{\ln q} \frac{d\ln q}{d\bar{T}_{as}} \right) \\ 15 &\quad + \left(K_a \frac{da}{d\bar{T}_{as}} \right) + \lambda_c + \text{Re} \end{aligned} \quad (3)$$

where the temperature feedback has been separated into the Planck feedback (the vertically uniform tropospheric warming equal to the surface warming) and the lapse rate feedback (the deviation from the tropospheric uniform warming):

$$\begin{aligned} \lambda_T &= \lambda_p + \lambda_{lr} = \left(K_{T_s} \frac{dT_s}{d\bar{T}_{as}} + K_T \frac{dT_s}{d\bar{T}_{as}} \right) \\ &\quad + \left(K_T \frac{dT}{d\bar{T}_{as}} - K_T \frac{dT_s}{d\bar{T}_{as}} \right) \end{aligned} \quad (4)$$

and where the water vapor feedback is computed assuming constant relative humidity (Soden et al., 2008; Shell et al., 2008; Jonko et al., 20 20).

In Eq. (3), K_x (the radiative kernel for a variable x) and x [temperature (T_s and T , in K), the natural logarithm of humidity ($\ln q$, in kg/kg) and the albedo (a , dimensionless)] are function of functions of the longitude, latitude, and pressure vertical coordinates in the monthly climatology. To obtain tropospheric averages, the water vapor and temperature feedbacks are vertically integrated from the surface up to the tropopause, defined as being 100 hPa in at the Equator, and varying linearly to 300 25 hPa in at the Poles. The stratospheric temperature and water changes is not accounted for in calculating the feedbacks, and they are shifted to the residuum.

We used both GFDL and National Center for Atmospheric Research (NCAR) radiative kernels to estimate climate feedbacks. More details on how the radiative kernels are obtained can be found in Soden et al. (2008) and Shell et al. (2008). It is worth noting that in the regression method, the radiative feedback is consistent with the actual radiative transfer scheme used in the climate model, while in the radiative kernel, the feedback is not necessarily consistent. In fact, the kernel is obtained from another climate model that is not among the models analyzed. Model intercomparison is easily achieved via this method, as the same kernel can be applied to all models (Soden and Held, 2006; Soden et al., 2008). This approach, however, assumes that the kernel is independent of the models and climate states and that uncertainties in the radiative transfer code used to compute them are small compared to the models' climate responses (Soden et al., 2008).

Due to the non-linearities involving clouds and net radiation at the TOA (Soden et al., 2008), the cloud feedback is not calculated directly from these radiative kernels, which represents one of the key limitations of the kernel method. Instead, the cloud feedback is approximated using the cloud radiative forcing (ΔCRE) corrected for by removing the non-cloud feedbacks effect as in Soden et al. (2004, 2008). After the calculation of non-cloud feedbacks for both all-sky and clear-sky (superscript cs) conditions, we thus estimate the cloud feedback (λ_c) as:

$$\Delta\text{CRE} = \Delta R - \Delta R^{cs}$$

$$\Delta\text{CRE}_k = (G - G^{cs})_{CO_2} - \Delta \bar{T}_{as} \sum_x (\lambda_x - \lambda_x^{cs})$$

$$\Delta\text{CRE}_a = \Delta\text{CRE} - \Delta\text{CRE}_k$$

$$\lambda_c = \frac{\Delta\text{CRE}_a}{\bar{T}_{as}} \quad (5)$$

Where, ΔR^{cl} is the clear-sky net radiation flux at the TOA. Following Soden et al. (2008), $(G - G_{cl})_{CO_2}$ was considered being equal to defined as $2 \times 0.69 \text{ W m}^{-2}$. The index “ k ” represents the change in the ΔCRE due to the non-cloud feedbacks, while the index “ a ” means the adjusted ΔCRE . Finally, a 30-year mean relative to the period from the 120th to 150th year of each scenario was used for all feedbacks estimation feedback estimations.

3.3 Changes in the atmospheric circulation and precipitation

Monthly mean climatologies are were computed for the last 30 years of the piControl and abrupt4xCO₂ runs, and the projected climate response to CO₂ increase is was evaluated from the difference between these abrupt4xCO₂ and piControl monthly mean climatologies. The statistical significance of this difference is was calculated based on the t-Student test. The significance level used is Student t-test with a significance level of 90%. Furthermore, in order to evaluate how similar two spatial pattern patterns are, we used the spatial inner product calculated as $\sum(A_i \cdot B_i) / (|A| \cdot |B|)$, where A and B are the 2-D variables and i is the spatial index related to their lat-lon coordinates.

4 Results

4.1 G , λ , ΔCRE and ECS estimated by ~~via the~~ Gregory method

Figure 1 shows the linear regressions of ΔR , ΔLW (clear-sky) and ΔSW (clear-sky) against $\Delta\bar{T}_{as}$ ~~for from~~ BESM. These linear regressions, ~~which are~~ based on all-sky data, ~~are~~ used to estimate ECS, G and λ , ~~here in Figure 1 and~~ the regressions are 5 also based on clear-sky data to obtain ΔCRE (as mentioned in the previous section). BESM features $G = 8.62 \text{ W m}^{-2}$, $\lambda = -1.45 \text{ W m}^{-2} \text{ K}^{-1}$, $\Delta\text{CRE} = -0.13 \text{ W m}^{-2} \text{ K}^{-1}$, and ECS = 2.96 K.

The parameters G , λ , ΔCRE and ECS ~~as~~ computed for all models are shown in Table 3. The climate sensitivities of ~~the~~ 26 CMIP5 coupled models (including BESM-OA2.5) were assessed as ~~it was previously~~ performed by Andrews et al. (2012) for 15 CMIP5 coupled models. In the present work, we ~~included added~~ the following models: ACCESS1-0, ACCESS1-3, 10 bcc-csm1-1, BESM-OA2.5, BNU-ESM, CCSM4, FGOALS-g2, FGOALS-s2, GISS-E2-H, GISS-E2-R, ~~e and~~ inmcm4. For the 15 ~~same models~~ ~~models used in Andrews et al. (2012)~~, we found similar results ~~to those of Andrews et al. (2012), which range between~~ ~~in which the ECS ranges, on average, from~~ 2.07 to 4.74 K. The ~~possibly small differences we attribute possible~~ ~~small differences can be attributed~~ to the interpolation of the data ~~as detailed in previous section~~. G and λ vary from 5.01 to 8.95 W m^{-2} and from -1.66 to -0.60 $\text{W m}^{-2} \text{ K}^{-1}$, respectively. ~~Inter-model~~ ~~The inter-model~~ spread in G among the models 15 ~~are is~~ due to differences in the radiative codes used, as well as ~~the due to~~ rapid adjustment processes ~~of in~~ the troposphere and ~~at the~~ surface (Collins et al., 2006; Gregory and Webb, 2008; Andrews and Forster, 2008). The spread in the ECS is more ~~robustly~~ influenced by λ than ~~by~~ G (Figure 2), as was also suggested by Andrews et al. (2012). The correlation coefficient between ~~the~~ ECS and λ is -0.82, which is significant at ~~a 1% of confidence interval significance level~~ (Figure 2b). On the other 20 hand, the correlation between ~~the~~ ECS and G is -0.01, ~~with which~~ is not statistically significant (Figure 2a). Thus, the ratio of climate restoration (associated with λ) ~~better~~ explains the dispersion in ~~ECS the ECS better~~ than the initial radiative imbalance triggered by the CO₂ increase (related to G). ~~Despite BESM presenting~~ ~~Although BESM yielded~~ one of the highest G ~~among all values among all of~~ the CMIP5 models, it ~~shows a response to doubling~~ ~~showed a warming response to~~ CO₂, ~~which is inside the warming doubling that is within the~~ range of $3.30 \pm 0.76 \text{ K}$ ~~as presented by the models of the ensemble ensemble~~ models.

25 ~~The~~ ΔCRE ~~for from~~ BESM is $-0.13 \text{ W m}^{-2} \text{ K}^{-1}$, while ~~the~~ CMIP5 models ~~have yield~~ ΔCRE ~~varying values~~ ~~ranging~~ from -0.50 to 0.70 $\text{W m}^{-2} \text{ K}^{-1}$. ~~This~~ ~~Unlike the~~ ΔCRE_a , ~~this~~ term does not consider the masking effects of clouds as ~~the~~ ΔCRE_a ~~estimated by~~ ~~estimated via~~ the radiative kernel method (Eq. 5). Therefore, ~~the~~ ΔCRE cannot be interpreted ~~as to~~ ~~reflect~~ a change in the cloud properties alone.

4.2 Climate ~~Feedbacks~~ ~~Feedbacks~~ estimated by ~~Radiative Kernel~~ ~~via the radiative kernel~~ method

30 Figure 3 shows the global-mean feedbacks for lapse-rate, water vapor, lapse-rate plus water-vapor, albedo, and cloud (SW, LW, and total) for each CMIP5 model. Both radiative kernels are used to test whether the results are sensitive to the ~~particular~~ choice of radiative kernel, ~~and whether and whether the~~ inter-model differences are greater than the distribution of the radiatively active constituents of the base model. It is worth clarifying that positive/negative values of feedbacks contribute to

the amplification/damping of global warming. The strongest positive feedback (Figure 3) is due to the water vapor (mean value: $1.39 \text{ W m}^{-2} \text{ K}^{-1}$), followed by clouds (mean value: $0.96 \text{ W m}^{-2} \text{ K}^{-1}$), and then surface albedo (mean value: $0.32 \text{ W m}^{-2} \text{ K}^{-1}$). The Planck feedback global-mean is negative, with an average value of $-3.60 \text{ W m}^{-2} \text{ K}^{-1}$ (not shown in Figure 3) followed by, followed by a lapse-rate feedback with of $-0.77 \text{ W m}^{-2} \text{ K}^{-1}$. BESM yields values near the ensemble mean for the albedo and cloud feedbacks, i.e., $0.27 \text{ W m}^{-2} \text{ K}^{-1}$ and $0.95 \text{ W m}^{-2} \text{ K}^{-1}$, respectively. For the lapse-rate feedback BESM yields a value of $-0.71 \text{ W m}^{-2} \text{ K}^{-1}$, which is an overestimation compared to the ensemble mean value. In turn, BESM is among the models with the lowest global water vapor feedback average, with a value of around $1.24 \text{ W m}^{-2} \text{ K}^{-1}$.

For all of the models in Figure 4a-b, there is an almost a nearly constant Planck feedback about 4 of approximately $-3.4 \text{ W m}^{-2} \text{ K}^{-1}$ from 90°S to 60°N , with a notable increased increase in the ensemble standard deviation in the subantarctic latitude sub-Antarctic latitudes (around 60°S). The exception is in the Arctic regionwhere, where the mean value reaches $-10 \text{ W m}^{-2} \text{ K}^{-1}$ with almost nearly the same increased standard deviation .BESM in the subantartic value. In the sub-Antarctic and Arctic latitudespresented, BESM yields one of the lowest values for the Planck feedback, revealing that BESM has a stronger vertically homogeneous warming (with respect to the surface temperature) among the CMIP5 models. Furthermore, for those same region regions, BESM showed greater lapse-rate feedback, corroborating confirming that BESM does not have a higher contrast between the surface and upper troposphere temperatures as in comparison to temperature contrasts of the other models.

As described in Soden et al. (2008), both lapse-rate and water vapor feedbacks partially compensate each other. The stronger increase in upper troposphere temperature than near-surface temperature in all models (shown in Figure 4) results in a negative lapse-rate feedback in the Tropics. On the other hand, the high-latitude warming is more close to the surface In the Tropics, which reflect in a positive where there is an intense moist convection, atmospheric warming almost follows a moist adiabat (temperature increase is greater at the upper troposphere compared to that at the surface), implying a negative lapse-rate feedback. Considering the Clausius-Clapeyron relation, the upper troposphere with an increased temperature could allow more water vapor concentration, leading to a positive water vapor feedback. The opposite is also true, e.g. positive lapse-rate feedback could exist as a result of a lower warming and humidity at the upper troposphere than near the surface, which can be associated with a negative (Figure 4c-d) (Manabe and Stouffer, 1980). In accordance with this upper tropospheric warming in the Tropics, an increase in the specific humidity occurs (Manabe and Wetherald, 1975), which is responsible for a potentialization of the greenhouse gas effect, revealing a positive water vapor feedback. However, recently Po-Chedley et al. (2018) showed that the correlation between as shown in Figure 4d-e. Because of this link between the lapse-rate and water vapor feedbacks is more related to, it is common to sum their effects, as performed in Figure 3. BESM shows a lapse-rate feedback near the ensemble mean for the Tropics. The greatest BESM deviations are observed near the Antarctic and over the Arctic (Figure 4c-d), where this feedback became positive for all models. For the patter of surface warming than the covariation of the local tropical lapse-rate and water vapor feedbacks. For water vapor feedback it is observed a greater dispersion, greater dispersion of the models was observed in the Tropics, with BESM systematically presenting values below of yielding values below the ensemble mean for the same latitude band. This behavior extends (Figure 4e-f). These lower values extend throughout the Northern Hemisphere, consistent with the low global mean water vapor feedback value relative to the ensemble (shown in Figure 3).

The albedo feedback is important in regions values computed for BESM and other CMIP5 models are shown in Figure 4g-h. These results are particularly important over the Polar regions, where there is a reduction in sea-ice and snow cover near the Polar Regions (Figure 4). The positive signal of the albedo feedback implies albedo feedback signals yielded by all of the models in such regions imply that the reduction in the albedo corresponds to an increase in both the radiation budget at the TOA (due to the reduction of, due to reduced upward shortwave radiation) and temperature near the surface. The albedo feedback shows. As expected the Polar regions present a large dispersion among models in northern high latitudes. It is emphasized that not only the albedo feedback contributes to the Arctic Amplification. In fact, as discussed by Pithan and Mauritsen (2014), the albedo feedback is the second main contributor to Arctic Amplification, while the largest contributor is the temperature feedback. The explanation for the importance of temperature feedback during the the models, which is related to how fast the sea-ice cover melts in the different climate models. The regions over the Arctic and the ocean near the Antarctic showed the largest surface warming, is in the fact that more energy is radiated back to space in low latitudes, compared with the Arctic. BESM shows and this positive albedo, together with the positive lapse-rate feedbacks, are the main factor responsible for a phenomenon known as polar amplification (Pithan and Mauritsen, 2014). BESM yielded an albedo feedback greater than the ensemble standard deviation over Southern ocean the Southern Ocean at around 60°S. This same latitude is where Planck and BESM shows negative Planck and positive lapse-rate feedbacks are out of models limits for BESM. Also, as a consequence of sea-ice melting, that region experienced a stronger increase in atmosphere temperature comparatively to the ensemble spread. Those negative values are more evident over the Tropical Pacific and North Atlantic oceans outside of the models limits, as previously discussed.

Regarding cloud feedbacks Finally, regarding cloud feedback, most of the inter-model spread arise arises from the SW component (figures Figures 3 and 4i-j). This dispersion is also noted reflected in the standard deviation and in the limit between the minimum and maximum of the zonally averaged cloud feedback shown in Figure 4i-j. The SW cloud feedback ranges from -0.28 to 1.40 $\text{W m}^{-2} \text{K}^{-1}$, while the LW cloud effect ranges from 0.10 to 0.96 $\text{W m}^{-2} \text{K}^{-1}$. The combined SW and LW cloud effects result in a positive cloud feedback ranging from 0.35 to 1.69 $\text{W m}^{-2} \text{K}^{-1}$. This result is similar to that found by Soden et al. (2008) for CMIP3 [IPCC AR4, IPCC (2007)] models, where they presented a near as they reported a nearly neutral and positive cloud feedback. BESM presents positive values of around 0.5 $\text{W m}^{-2} \text{K}^{-1}$ for both SW and LW cloud feedback, which results resulting in a total cloud feedback of about 1.0 $\text{W m}^{-2} \text{K}^{-1}$ (as shown in Figure 3). The highest positive values are in regions with strong albedo feedback (Figure 4i-j).

Overall, BESM lies within the range of CMIP5 models, with global-mean values of $1.24 \text{ W m}^{-2} \text{K}^{-1}$, $0.95 \text{ W m}^{-2} \text{K}^{-1}$, $0.27 \text{ W m}^{-2} \text{K}^{-1}$. Although BESM yielded global area-averaged feedbacks near the model ensemble mean values, $-3.57 \text{ W m}^{-2} \text{K}^{-1}$ and $-0.71 \text{ W m}^{-2} \text{K}^{-1}$ for water vapor, cloud, albedo feedbacks, Planck and lapse-rate feedbacks, respectively. However, differences between BESM and the other models are found differences are found mainly in the high latitudes, where BESM exhibit lapse-rate and humidity feedbacks marginally out of range of values set by the CMIP5 multi-model ensemble (Figure 4). It is also evident from figures 4 and 5 that. In fact, for cloud feedback, BESM is an outlier for the cloud feedbacks. This is due to a strong shortwave component response over both the Arctic and the Southern Ocean near Antarctica. Considering the Antarctic. This effect is evident via the decomposition of the cloud feedback into the SW and LW components for the ensemble

and BESM values, as shown in Figure 5. To assess the causes of this strong BESM shortwave cloud feedback departure from the ensemble, we separately computed the contributors to the SW cloud feedback, i.e., the SW CRE [as described by Cess et al. (1989)] and the ~~individual components of feedback cloud mask, we can note that those higher values in cloud feedback~~ feedback cloud masks, as in Eq. (5). For the shortwave component, the feedback cloud masks are obtained for the albedo and SW water vapor feedbacks, performing the all-minus clear-sky radiation for each feedback. We observe that the higher BESM cloud feedback values (Figure 6g-h) are mainly consequences of the sum of ~~SW-CRE~~ the SW CRE (Figure 6a-b) and the effect of cloud masking for ~~albedo feedback~~ ($\lambda_a - \lambda_{ac}$), as the albedo feedback (Figure 6c-d) in the sub-Antarctic and Arctic regions. In turn, the cloud masking for the SW water vapor (Figure 6e-f) does not contribute to the higher positive BESM values. As shown in Figure 6. ~~For Arctic region~~, it is possible to see that the major contributor for BESM be an outlier to BESM's status as an outlier over the Arctic region is the SW CRE, while ~~for over the ocean near the Antarctic is in the~~ Southern Ocean (around 60°S), the major contribution comes from the albedo feedback cloud mask. In this latter, since the radiative kernel for both all-and clear-sky are the same throughout the models, the difference among them is the albedo change $\Delta a / \Delta \bar{T}_{as} (K_a - K_a^{cs})$

A further analysis to understand the BESM cloud feedback behavior in high latitudes is obtained by examining the zonal mean of the change in the cloud vertical profile for BESM, as shown in Figure 7. Over the ~~both regions~~ (Arctic and near Antarctic), the Antarctic, BESM showed an increase in the cloud fraction above 850 hPa and a decrease below that level ~~for BESM is observed, which means a~~ indicating an upward shift of low-level clouds ~~upward shifting~~. Moreover (Figure 7a). However, the increase in cloud cover above 850 hPa is stronger than the reduction below (Figure 7a). As consequence. Because of this increase in the total cloud fraction, a negative SW CRE ~~change is present~~ appears in those regions (~~but not stronger for BESM comparatively to other models~~), that is the response to the ~~Figure 6a-b~~, consistent with an increase in sun shading (Figure 7b). ~~However~~ Moreover, the SW cooling is smaller than the heating provided by LW radiation, ~~as presented due to the upward shift of the low-level clouds, as evident~~ in the net effect (Figure 7d). The net radiation heating change is more intense around 60°S, that can be related to the more intense surface albedo change, as well as the low-cloud lifting. Despite of the lost ~~Furthermore, the positive albedo and lapse-rate feedbacks (Figure 4c-f) are consistent with this vertical cloud shifting.~~ In this manner, a loss of SW energy at ~~surface (related to the increased sun shading)~~, which results in a SW cloud radiative effect ~~negative, it is overcome by~~ the surface associated with an increase in the total cloud fraction explains the negative SW CRE, and the gain of LW energy is responsible for the sea-ice melting. Consequently, this gain of LW energy is indirectly linked to the albedo feedback cloud mask, ~~that contribute to a cloud feedback positive over those two regions~~. for BESM, since the mask [$\Delta a / \Delta \bar{T}_{as} (K_a - K_a^{cs})$] is proportional to the albedo change (Δa). As discussed before, both the SW CRE and albedo feedback cloud mask contribute to the large, positive cloud feedback over the Arctic and sub-Antarctic areas observed in BESM.

4.3 Changes in temperature, atmospheric circulation and precipitation

Figure 8 shows the annual mean ~~for surface temperature change~~ surface temperature differences between the abrupt4xCO₂ and piControl scenarios for the ensemble of 25 CMIP5 models and BESM. ~~It is clearly seen~~ As clearly shown in Figure 8 that,

despite the generalized increase ~~of in~~ the air temperature over most of the globe in both panels, BESM shows a generally lower temperature increase, principally over the continental areas. The CMIP5 ensemble shows a mean continental temperature increase of 6.78 K, while BESM shows a value of 5.57 K. ~~Notwithstanding Nevertheless~~, the spatial ~~pattern of temperature increase is patterns of the temperature increases are~~ similar, as measured by the spatial inner product (as described in the 5 previous section) between the ~~two upper upper two~~ panels in Figure 8, which results in ~~the a~~ a value of 0.96 (values near 1 ~~mean indicate~~ that both variables have similar spatial pattern, whereas values near 0 mean that there are few spatial correspondences between variables). One point of interest ~~of within~~ the scientific community is the relative low temperature increase over the 10 subpolar North Atlantic, also ~~referred as referred as the~~ warming hole (Drijfhout et al., 2012). In the CMIP5 ensemble mean, the North Atlantic does not show a ~~decrease of temperature, but temperature decrease, although~~ it is the region with the smallest 15 temperature increase globally~~;~~ while BESM shows an area of temperature decrease in this region. Such a decrease is also present in ~~other~~ 6 ~~other~~ analyzed models (CSIRO-Mk3-6-0, FGOALS-s2, GFDL-ESM2G, GFDL-ESM2M, GISS-E2-R, and inmcm4). ~~This~~ ~~These~~ results are consistent with ~~Drijfhout et al. (2012), who those of Drijfhout et al. (2012), which~~ showed that both observations and CMIP5 models present maximum cooling in the center of the subpolar gyre. Those authors argue that there ~~are evidences that both is evidence that both the~~ subpolar gyre and ~~the~~ AMOC adjust in concert with different time 20 lags.

The regions with the largest temperature increase in the abrupt4xCO₂ scenario are the Polar ~~Regions~~ ~~regions~~, mainly over the North Pole. The equatorial Pacific shows an increase in temperature ~~in when~~ the abrupt4xCO₂ scenario ~~when is~~ compared with the piControl, both in the CMIP5 ensemble and BESM. Such changes in the Pacific mean state ~~is in line are consistent~~ with the IPCC-AR5, ~~in which it is shown which reports~~ that the Pacific Ocean becomes warmer near the equator compared to the 25 subtropics in the CMIP5 projections (Liu et al., 2005; Gastineau and Soden, 2009; Cai et al., 2015). The scatter plot of ~~global average of the global average under the abrupt4xCO₂ versus piControl conditions versus the piControl conditions~~ presented in Figure 8 ~~is an provides~~ additional information that helps to understand the ~~models~~ dispersion around the mean value ~~among the different models~~. Even though ~~there is a predominance of models in either quadrants the outputs of most of the models lie in either quadrant 1 or 3 (top-right and bottom-left, respectively), it is not possible to note a linear relationship. It means This 30 result indicates~~ that models with warmer/cooler mean climates in the piControl runs ~~aparently does not present apparently do not show a corresponding warmer/cooler climate for in~~ the abrupt4xCO₂ experiments.

~~BESM yields a temperature near that of the ensemble in both the piControl and abrupt4xCO₂ runs; consequently, it also showed a temperature increase near the ensemble mean, consistent with its Plank feedback (Figures 3 and 4a-b).~~

Figure 9 shows the precipitation changes between ~~the~~ abrupt4xCO₂ and piControl scenarios for ~~the~~ multi-model ensemble 30 and ~~the~~ BESM. The results are approximately similar to ~~those of~~ Held and Soden (2006), with wet regions becoming wetter (near-equatorial and subpolar regions) and dry regions becoming drier (centered around 30° in both hemispheres). The precipitation pattern in the CMIP5 ensemble ~~has shows~~ increased precipitation over the equatorial Pacific, which ~~ean could~~ be related to the equatorial Pacific warming pattern shown in the temperature change (Figure 8). ~~Also~~ ~~Furthermore~~, the CMIP5 ensemble shows a decrease in precipitation in northern South America. ~~The~~ BESM precipitation pattern is similar to the spatial patterns 35 in the CMIP5 ensemble, ~~yet but~~ with some notable discrepancies. For example, the ~~deerease in decreased~~ precipitation over

the South Pacific shown in the CMIP5 ensemble plot is extended into the Indonesian region in BESM. It is also worth noting that in the BESM simulation the South Pacific convergence zone (SPCZ) shifts southward in the abrupt4xCO₂ scenario, compared to piControl. Over South America scenario, compared with its position in the piControl scenario. In both the multi-model ensemble and BESM, the precipitation change pattern over South America is similar to that which occurs during El Niño years (Kayano et al., 1988; Marengo and Hastenrath, 1993; Grimm and Tedeschi, 2009), with increased precipitation over southeastern South America and decreased precipitation over northern/northeastern South America, in both the multi-model ensemble and BESM. The scatter plot in Figure 9 suggests a linear relationship between experiments, meaning that models that have a larger (smaller) precipitation change in the piControl scenario show a larger (smaller) precipitation change in the abrupt4xCO₂ scenario. In the scatter plot of As shown in Figure 9, BESM has value the BESM value is near the center of the scatter plot, which means that it presents yields global averaged precipitation values similar to the average of all of the models used in the ensemble.

Figure 10 depicts the shows a scatter plot of the ECS versus the change in precipitation between precipitation difference between the Abrupt4xCO₂ and piControl scenarios (ΔP_r), for all models considered for all of the considered models. It is worth noting that all the models present show increased global-mean precipitation for the upon quadrupling of atmospheric CO₂ with piControl pre-industrial CO₂ concentrations (positive values in y-axis in Figure 10). The apparent linear relationship between these differences (abrupt4xCO₂ minus piControl) in the global-mean precipitation and ECS is also evident in Figure 10, in which the warmest models tend to have highest changes in precipitation the largest precipitation changes. The slope of the linear regression is reflects a 2.5% of precipitation change per K, which is close to that found by Held and Soden (2006). This slope is much inferior to that expected for lower than that predicted by the Clausius-Clapeyron relation, which is about 6, 5% of precipitation change i.e., an approximately 6.5% change in precipitation per K. In fact, precipitation increasing is such precipitation increases are not governed by the availability of moisture but moisture availability but rather by the surface and tropospheric energy balance, including in this process which incorporates the surface radiative heating, surface latent heat flux and radiative cooling of the troposphere (Allen and Ingram, 2002).

MRI-CGCM3, ACCESS1-0, and HadGEM2-ES show greater deviation deviations from the linear fit shown in Figure 10. Also Furthermore, BESM is marginally out of the residual standard error interval, with a 9.5% increased increase in precipitation (the error limit is 9.2%). ACCESS1-0 and HadGEM2-ES use the same atmospheric model (Bi et al., 2013; Dix et al., 2013), which could explain the lower increase in precipitation in both coupled models.

As in the case of In addition to temperature and precipitation changes, we are also interested in understanding the alteration changes in the BESM atmospheric circulation (compared to other models) considering following a quadrupling of the CO₂ concentration. The sea level pressure (SLP) response patterns shown in Figure 11 depict a poleward shift of the subtropical high pressure cells for in the subtropical high-pressure cells in both the CMIP5 ensemble and BESM. Furthermore, when the models are subjected to the increase of increased atmospheric CO₂ concentration, a decrease in the SLP over the Polar regions is evident. This SLP decrease over the Polar regions and the increase in the mid-latitudes indicate a positive trend of Arctic Oscillation in Arctic oscillation (AO) and Antarctic Oscillation oscillation (AAO) episodes, which have already been reported in the studies of by Fyfe et al. (1999), Cai et al. (2003), and Miller et al. (2006). It is also interesting to note the statistically

significant SLP decrease (increase) over the eastern (western) Pacific, a pattern that might be indicative of indicate an ENSO-like pattern in scenarios with an increased CO₂ concentration. This pattern is coherent consistent with those depicted in Figure 8 for the SST changes in a 4xCO₂ scenario.

Results for The results from the piControl scenario (the contours in Figure 12) show that the Southern Hemisphere sub-tropical jet, depicted reflected by the core of the maximum eastward zonal wind, is localized around 35°S, 200-150 hPa, in both the CMIP5 ensemble and BESM. We note that In both panels of Figure 12 (BESM and the CMIP5 ensemble), we note that the regions with the strongest positive values (anomalous eastward wind) in increases in westerly winds at all levels show a southward displacement in both panels of Figure 12 (BESM and the CMIP5 ensemble). This jet displacement. This observation is consistent with the poleward displacement of the high SLP center shown in Figure 11. Also Furthermore, as the high-pressure centers experienced a poleward shift, the pressure gradients are intensified in intensified in the subpolar areas, and consequently increased consequently, the near-surface wind velocity is a result increased, following the geostrophic approximation [$u \approx -(1/f\rho)(\partial p/\partial y)$], where f is the Coriolis parameter and ρ is the air density.

Figure 13 shows the average differences from 5°N – 5°S (Walker circulation) differences between between the abrupt4xCO₂ and piControl scenarios for omega (shades) and zonal wind and vertical velocity omega vertical motion (vectors). According to the pattern of omega in omega pattern in the piControl (contours), the multi-model ensemble and BESM show subsidence over an extensive area in the Pacific (150°E – 90°W), which intensity is reduced whose intensity is lower in the abrupt4xCO₂ simulation, as indicated shown in Figure 13 (blue). This finding is coherent with near-surface temperature patterns (Figure 8), which show an equatorial warming pattern in the mean state (e.g., during El Niño years, a weakening of the Walker circulation occurs). Furthermore, there are positive values in for the difference between the two scenarios over South America (around 75°W), consistent with the decrease of in precipitation in tropical South America, in both BESM and the CMIP5 ensemble (Figure 9).

5 Conclusions

The piControl and abrupt4xCO₂ scenarios for 25 CMIP5 models have been contrasted compared with those generated by the BESM-OA2.5 BESM model, based on their climate sensitivity parameters, such as the Equilibrium Climate Sensitivity equilibrium climate sensitivity (ECS) and climate feedbacks. Also, the Furthermore, changes in the temperature, atmospheric circulation and precipitation patterns were investigated.

Applying the linear regression method (Gregory et al., 2004), we obtain ECS obtained the ECS values for the 25 CMIP5 models analyzed ranging, which ranged from 2.07 to 4.74 K, with BESM showing 2.96 K, close to the ensemble mean value (3.30 ± 0.76). BESM has one of the biggest radiative forcing (G) with 8, 62 values, i.e., $8.62 \text{ W m}^{-2} \text{ K}^{-1}$, which is related to the radiative code transference transfer model and the rapid adjustment process (Collins et al., 2006; Gregory and Webb, 2008; Andrews and Forster, 2008). Both G and the climate sensitivity (λ) define the ECS values calculated with this method, however, only λ presents shows a significant correlation with the ECS, corroborating with Andrews et al. (2012) results the results of Andrews et al. (2012).

To go further in the analysis, the radiative kernel method ~~is was~~ used to separate the climate feedback into Planck, lapse-rate, water vapor, albedo and cloud feedbacks. Two regions presented considerable standard ~~deviation for Plank~~ ~~deviations for the Planck~~, lapse-rate and albedo ~~values, i.e.,~~ the Arctic region and over the ocean near the Antarctic. Over ~~those regions, BESM-OA2.5 also shows these regions, BESM also showed~~ cloud feedback values larger than the zonal mean plus ~~the~~ standard deviation for the analyzed models, reaching ~~near approximately~~ $3 \text{ W m}^{-2} \text{ K}^{-1}$, while the zonal mean ~~is around was approximately~~ $0 \text{ W m}^{-2} \text{ K}^{-1}$. For BESM-OA2.5 was observed a shift upward BESM showed an upward shift of the low-cloud cover and an increase in cloud cover between 850 and 700 hPa, ~~what is responsible for a and these features were responsible for~~ sun shading at ~~surface, increasing the surface, which increased~~ the outgoing SW radiation at the TOA. Moreover, BESM-OA2.5 BESM presented a greater albedo change ~~than compared with those of the~~ other models, ~~specially in the subantarctic especially in the sub-Antarctic~~ area. Despite of the ~~lost loss~~ of SW energy at surface, which results in a negative SW cloud radiative effect, ~~it is this effect was~~ overcome by the albedo feedback cloud mask, ~~that contribute to a which contributes to~~ positive cloud feedback over those regions.

~~Atmospheric~~ The atmospheric circulation patterns in BESM-OA2.5 are similar to patterns in BESM were similar to the patterns of the multi-model ensemble and in those of other studies regarding the near-surface temperature (IPCC, 2007, 2013). For precipitation, the thermodynamic component evidences reflects the well-known ‘wet-gets-wetter’ and ‘dry-gets-drier’ pattern of precipitation changes (Held and Soden, 2006). BESM-OA2.5 along with patterns of precipitation change (Held and Soden, 2006). BESM as well as the CMIP5 ensemble have show consistent weakening of the Walker circulation, principally in the Pacific and over northern South America, which has been reported in previous studies (Collins et al., 2010; DiNezio et al., 2012; Huang and Xie, 2015; Cai et al., 2015). Regarding SLP, both BESM and the CMIP5 ensemble indicate a poleward displacement of the subtropical high pressure high-pressure systems, as shown in other studies (Fyfe et al., 1999; Cai et al., 2003; Miller et al., 2006). In line with such displacement, the subtropical jet is also shifted polewards, and it is more evident this effect was clearer in the Southern Hemisphere.

BESM-OA2.5 BESM is an additional climate model with ability of reproduce changes that are physically understood in order that can reproduce physically understood changes to study the global climate system. In this sense, the BESM results contributed to better understand its use has contributed to a better understanding of the inter-model spread in cloud feedback. Furthermore, BESM is under development in order to overcome the present extra-tropical and tropical climate simulation deficiencies, as reported in Casagrande et al. (2016) and Veiga et al. (2019a), respectively.

Notwithstanding, the BESM Development Team is committed to improving the cloud cover of the model as well as its land surface model in subsequent versions. Furthermore, it is important to mention that the radiative energy imbalance of -4 W m^{-2} at the TOA, arising from our ocean-atmosphere coupling, is under revision. We hope that the next version will include improved energy flows diagnostics and that it will be more compatible physical parameterizations between the ocean and atmosphere.

Code and data availability

The BESM-OA2.5 source code is freely available ~~after signature of subject to~~ a license agreement. Please contact Paulo Nobre to obtain the [BESM-OA2.5](#) source code and data ~~of BESM-OA2.5~~.

Competing interests. The authors declare that they have no conflict of interest.

5 *Acknowledgements.* This work ~~is supported by~~was supported by the Sao Paulo Research Foundation (FAPESP, 2009/50528-6, 2014/50848-9 and 2018/06204-0), the National Coordination for High Level Education and Training (CAPES, Grant 16/2014), the CAPES/National Water Agency (CAPES/ANA, 88887.115872/2015-01), the Brazilian National Council for Scientific and Technological Development (CNPq, 490237/2011-8 and 302218/2016-5), the Brazilian Research Network on Global Climate Change (FINEP/Rede Clima, Grant 01.13.0353-00), the National Institute for Science and Technology on Climate Change (INCT-MC 573797/2008-0), and INCT-MC Phase 2 funded by CNPq
10 (Grant 465501/2014-1).

References

Allen, M. R. and Ingram, W. J.: Constraints on future changes in climate and the hydrologic cycle, *Nature*, 419, 224–232, <https://doi.org/10.1038/nature01092>, 2002.

Alpert, J. C., Kanamitsu, M., Caplan, P. M., Sela, J. G., White, G. H., and Kalnay, E.: Mountain induced gravity wave drag parameterization in the NMC medium-range forecast model, pp. 726–733, Amer. Metero. Soc., 1988.

5 Amaya, D. J., DeFlorio, M. J., Miller, A. J., and Xie, S.-P.: WES feedback and the Atlantic Meridional Mode: observations and CMIP5 comparisons, *Climate Dynamics*, 49, 1665–1679, <https://doi.org/10.1007/s00382-016-3411-1>, 2017.

Andrews, T. and Forster, P. M.: CO₂ forcing induces semi-direct effects with consequences for climate feedback interpretations, *Geophysical Research Letters*, 35, <https://doi.org/10.1029/2007GL032273>, 2008.

10 Andrews, T., Gregory, J. M., Webb, M. J., and Taylor, K. E.: Forcing, feedbacks and climate sensitivity in CMIP5 coupled atmosphere-ocean climate models, *Geophysical Research Letters*, 39, n/a–n/a, <https://doi.org/10.1029/2012GL051607>, 2012.

Arrhenius, S.: On the influence of carbonic acid in the air upon the temperature of the ground., vol. 41, 1896.

Arya, S. P.: *Introduction to Micrometeorology*, Academic Press, 1988.

Bi, D., Dix, M., Marsland, S., O'Farrell, S., Rashid, H., Uotila, P., Hirst, T., Kowalczyk, E., Golebiewski, M., Sullivan, A., Yan, H., Hannah, 15 N., Franklin, C., Sun, Z., Vohralik, P., Watterson, I., Zhou, X., Fiedler, R., Collier, M., Ma, Y., Noonan, J., Stevens, L., Uhe, P., Zhu, H., Griffies, S., Hill, R., Harris, C., and Puri, K.: The ACCESS Coupled Model: Description, Control Climate and Evaluation, *Australian Meteorological and Oceanographic Journal*, 63, 41–64, 2013.

Bony, S., Colman, R., Kattsov, V. M., Allan, R. P., Bretherton, C. S., Dufresne, J. L., Hall, A., Hallegatte, S., Holland, M. M., Ingram, W., Randall, D. a., Soden, B. J., Tselioudis, G., and Webb, M. J.: How well do we understand and evaluate climate change feedback processes?, <https://doi.org/10.1175/JCLI3819.1>, 2006.

20 Businger, J. A., Wyngaard, J. C., Izumi, Y., and Bradley, E. F.: Flux-Profile Relationships in the Atmospheric Surface Layer, *Journal of the Atmospheric Sciences*, 28, 181–189, [https://doi.org/10.1175/1520-0469\(1971\)028<0181:FPRITA>2.0.CO;2](https://doi.org/10.1175/1520-0469(1971)028<0181:FPRITA>2.0.CO;2), 1971.

Cai, W., Whetton, P. H., and Karoly, D. J.: The Response of the Antarctic Oscillation to Increasing and Stabilized Atmospheric CO₂, *Journal of Climate*, 16, 1525–1538, <https://doi.org/10.1175/1520-0442-16.10.1525>, 2003.

25 Cai, W., Santoso, A., Wang, G., Yeh, S.-W., An, S.-I., Cobb, K. M., Collins, M., Guilyardi, E., Jin, F.-F., Kug, J.-S., Lengaigne, M., McPhaden, M. J., Takahashi, K., Timmermann, A., Vecchi, G., Watanabe, M., and Wu, L.: ENSO and greenhouse warming, *Nature Climate Change*, 5, 849–859, <https://doi.org/10.1038/nclimate2743>, 2015.

Caldwell, P. M., Zelinka, M. D., Taylor, K. E., and Marvel, K.: Quantifying the Sources of Intermodel Spread in Equilibrium Climate Sensitivity, *Journal of Climate*, 29, 513–524, <https://doi.org/10.1175/JCLI-D-15-0352.1>, 2016.

30 Callendar, G.: The Artificial Production of Carbon Dioxide, *Quarterly Journal of the Royal Meteorological Society*, 64, 223–240, <https://doi.org/10.1002/qj.49706427503>, 1938.

Casagrande, F., Nobre, P., de Souza, R. B., Marquez, A. L., Tourigny, E., Capistrano, V., and Mello, R. L.: Arctic Sea Ice: Decadal Simulations and Future Scenarios Using BESM-OA, *Atmospheric and Climate Sciences*, 06, 351–366, <https://doi.org/10.4236/acs.2016.62029>, 2016.

Cess, R. D., Potter, G. L., Blanchet, J. P., Boer, G. J., Ghan, S. J., Kiehl, J. T., Le Treut, H., Li, Z.-X., Liang, X.-Z., Mitchell, J. F. B., 35 Morcrette, J.-J., Randall, D. A., Riches, M. R., Roeckner, E., Schlese, U., Slingo, A., Taylor, K. E., Washington, W. M., Wetherald, R. T., and Yagai, I.: Interpretation of Cloud-Climate Feedback as Produced by 14 Atmospheric General Circulation Models, *Science*, 245, 513–516, <https://doi.org/10.1126/science.245.4917.513>, 1989.

Cess, R. D., Potter, G. L., Blanchet, J. P., Boer, G. J., and Del Genio, a. D.: Intercomparison and interpretation of climate feedback processes in 19 atmospheric general circulation models, *Journal of Geophysical Research*, 95, 16 601–16 615, <https://doi.org/10.1029/JD095iD10p16601>, 1990.

Collins, M., An, S.-I., Cai, W., Ganachaud, A., Guilyardi, E., Jin, F.-F., Jochum, M., Lengaigne, M., Power, S., Timmermann, A., Vecchi, G., and Wittenberg, A.: The impact of global warming on the tropical Pacific Ocean and El Niño, *Nature Geoscience*, 3, 391–397, <https://doi.org/10.1038/ngeo868>, 2010.

Collins, W. D., Ramaswamy, V., Schwarzkopf, M. D., Sun, Y., Portmann, R. W., Fu, Q., Casanova, S. E. B., Dufresne, J.-L., Fillmore, D. W., Forster, P. M. D., Galin, V. Y., Gohar, L. K., Ingram, W. J., Kratz, D. P., Lefebvre, M.-P., Li, J., Marquet, P., Oinas, V., Tsushima, Y., Uchiyama, T., and Zhong, W. Y.: Radiative forcing by well-mixed greenhouse gases: Estimates from climate models in the Intergovernmental Panel on Climate Change (IPCC) Fourth Assessment Report (AR4), *Journal of Geophysical Research*, 111, <https://doi.org/10.1029/2005JD006713>, 2006.

Cubasch, U. and Cess, R. D.: Processes and modeling. *Climate Change: The IPCC Scientific Assessment*, Cambridge University Press, 1990.

DiNezio, P. N., Kirtman, B. P., Clement, A. C., Lee, S.-K., Vecchi, G. A., and Wittenberg, A.: Mean Climate Controls on the Simulated Response of ENSO to Increasing Greenhouse Gases, *Journal of Climate*, 25, 7399–7420, <https://doi.org/10.1175/JCLI-D-11-00494.1>, 2012.

Dix, M., Vohralik, P., Bi, D., Rashid, H., Marsland, S., O'Farrell, S., Uotila, P., Hirst, T., Kowalczyk, E., Sullivan, A., Yan, H., Franklin, C., Sun, Z., Watterson, I., Collier, M., Noonan, J., Rotstayn, L., Stevens, S., Uhe, P., and Puri, K.: The ACCESS coupled model: description, control climate and evaluation, *Australian Meteorological and Oceanographic Journal*, 63, 83–99, 2013.

Drijfhout, S., van Oldenborgh, G. J., and Cimatoribus, A.: Is a Decline of AMOC Causing the Warming Hole above the North Atlantic in Observed and Modeled Warming Patterns?, *Journal of Climate*, 25, 8373–8379, <https://doi.org/10.1175/JCLI-D-12-00490.1>, 2012.

Dufresne, J.-L. and Bony, S.: An Assessment of the Primary Sources of Spread of Global Warming Estimates from Coupled Atmosphere–Ocean Models, *Journal of Climate*, 21, 5135–5144, <https://doi.org/10.1175/2008JCLI2239.1>, 2008.

Eyring, V., Bony, S., Meehl, G. A., Senior, C. A., Stevens, B., Stouffer, R. J., and Taylor, K. E.: Overview of the Coupled Model Intercomparison Project Phase 6 (CMIP6) experimental design and organization, *Geoscientific Model Development*, 9, 1937–1958, <https://doi.org/10.5194/gmd-9-1937-2016>, 2016.

Ferrier, B. S., Jin, Y., Lin, Y., Black, T., Rogers, E., and DiMego, G.: Implementation of a new grid-scale cloud and precipitation scheme in the NCEP Eta Model, pp. 280–283, Amer. Meteor. Soc., 2002.

Figueroa, S. N., Kubota, P. Y., Grell, G., Morrison, H., Bonatti, J. P., Barros, S., Fernandez, J. P., Ramirez, E., Siqueira, L., Satyamurti, P., Luzia, G., da Silva, J., da Silva, J., Pendharkar, J., Capistrano, V. B., Alvin, D., Enore, D., Denis, F., Rozante, J. R., Cavalcanti, I., Barbosa, H., Mendes, C., and Tarassova, T.: The Brazilian Global Atmospheric Model (BAM). Part I: Performance for Tropical Rainfall forecasting and sensitivity to convective schemes and horizontal resolutions, *Weather and Forecasting*, 31, 1547–1572, <https://doi.org/10.1175/WAF-D-16-0062.1>, 2016.

Foley, J. a., Prentice, I. C., Ramankutty, N., Levis, S., Pollard, D., Sitch, S., and Haxeltine, a.: An integrated biosphere model of land surface processes, terrestrial carbon balance, and vegetation dynamics, vol. 10, 1996.

Fyfe, J. C., Boer, G. J., and Flato, G. M.: The Arctic and Antarctic oscillations and their projected changes under global warming, *Geophysical Research Letters*, 26, 1601–1604, <https://doi.org/10.1029/1999GL900317>, 1999.

Gastineau, G. and Soden, B. J.: Model projected changes of extreme wind events in response to global warming, *Geophysical Research Letters*, 36, <https://doi.org/10.1029/2009GL037500>, 2009.

Good, P., Andrews, T., Chadwick, R., Dufresne, J.-L., Gregory, J. M., Lowe, J. A., Schaller, N., and Shiogama, H.: nonlinMIP contribution to CMIP6: model intercomparison project for non-linear mechanisms: physical basis, experimental design and analysis principles (v1.0), *Geoscientific Model Development*, 9, 4019–4028, <https://doi.org/10.5194/gmd-9-4019-2016>, 2016.

5 Gregory, J. and Webb, M.: Tropospheric Adjustment Induces a Cloud Component in CO₂ Forcing, *Journal of Climate*, 21, 58–71, <https://doi.org/10.1175/2007JCLI1834.1>, 2008.

Gregory, J. M., Ingram, W. J., Palmer, M. A., Jones, G. S., Stott, P. A., Thorpe, R. B., Lowe, J. A., Jonhs, T. C., and Williams, K. D.: A new method for diagnosing radiative forcing and climate sensitivity, *Geophysical Research Letters*, 31, L03 205, <https://doi.org/10.1029/2003GL018747>, 2004.

10 Grell, G. A. and Dévényi, D.: A generalized approach to parameterizing convection combining ensemble and data assimilation techniques: PARAMETERIZING CONVECTION COMBINING ENSEMBLE AND DATA ASSIMILATION TECHNIQUES, 29, 38–1–38–4, <https://doi.org/10.1029/2002GL015311>, <http://doi.wiley.com/10.1029/2002GL015311>, 2002.

Griffies, S. M., Harrison, M. J., Pacanowski, Ronald, C., and Rosati, A.: A Technical Guide to MOM4, GFDL Ocean Group Technical Report No. 5, NOAA/Geophysical Fluid Dynamics Laboratory, p. Available online at www.gfdl.noaa.gov, 2004.

15 Grimm, A. M. and Tedeschi, R. G.: ENSO and Extreme Rainfall Events in South America, *Journal of Climate*, 22, 1589–1609, <https://doi.org/10.1175/2008JCLI2429.1>, 2009.

Harshvardhan, Davies, R., Randall, D. A., and Corsetti, T. G.: A fast radiation parameterization for atmospheric circulation models, *Journal of Geophysical Research*, 92, 1009, <https://doi.org/10.1029/JD092iD01p01009>, 1987.

Held, I. M. and Soden, B. J.: Robust Responses of the Hydrological Cycle to Global Warming, *Journal of Climate*, 19, 5686–5699, <https://doi.org/10.1175/JCLI3990.1>, 2006.

20 Holtslag, a. a. M. and Boville, B. a.: Local versus nonlocal boundary-layer diffusion in a global climate model, vol. 6, 1993.

Huang, P. and Xie, S.-P.: Mechanisms of change in ENSO-induced tropical Pacific rainfall variability in a warming climate, *Nature Geoscience*, 8, 922–926, <https://doi.org/10.1038/ngeo2571>, 2015.

Iacono, M. J., Delamere, J. S., Mlawer, E. J., Shephard, M. W., Clough, S. A., and Collins, W. D.: Radiative forcing by long-lived greenhouse gases: Calculations with the AER radiative transfer models, *Journal of Geophysical Research*, 113, <https://doi.org/10.1029/2008JD009944>, 25 2008.

IPCC: Climate change 2007: the physical science basis; contribution of Working Group I to the Fourth Assessment Report of the Intergovernmental Panel on Climate Change, 2007.

IPCC: Climate change 2013: the physical science basis; Working Group I contribution to the Fifth Assessment Report of the Intergovernmental Panel on Climate Change, 2013.

30 Jiménez, P. a., Duhdia, J., González-Rouco, J. F., Navarro, J., Montávez, J. P., and García-Bustamante, E.: A Revised Scheme for the WRF Surface Layer Formulation, *Monthly Weather Review*, 140, 898–918, <https://doi.org/10.1175/MWR-D-11-00056.1>, 2012.

Jonko, A. K., Shell, K. M., Sanderson, B. M., and Danabasoglu, G.: Climate Feedbacks in CCSM3 under Changing CO₂ Forcing. Part II: Variation of Climate Feedbacks and Sensitivity with Forcing, *Journal of Climate*, 26, 2784–2795, <https://doi.org/10.1175/JCLI-D-12-00479.1>, 2013.

35 Kanamitsu, M., Ebisuzaki, W., Woollen, J., Yang, S.-K., Hnilo, J. J., Fiorino, M., and Potter, G. L.: NCEP–DOE AMIP-II Reanalysis (R-2), *Bulletin of the American Meteorological Society*, 83, 1631–1643, <https://doi.org/10.1175/BAMS-83-11-1631>, 2002.

Kaplan, L. D.: The Influence of Carbon Dioxide Variations on the Atmospheric Heat Balance, *Tellus*, 12, 204–208, <https://doi.org/10.1111/j.2153-3490.1960.tb01301.x>, 1960.

Kayano, M. T., Rao, V. B., and Moura, A. D.: Tropical circulations and the associated rainfall anomalies during two contrasting years, *Journal of Climatology*, 8, 477–488, <https://doi.org/10.1002/joc.3370080504>, 1988.

Kubota, P. Y.: Variability of stored energy in the surface and its impact on the definition of the precipitation pattern over South America (Variabilidade de energia armazenada na superfície e seu impacto na definição do padrão de precipitação na América do Sul), Ph.D. thesis, 5 National Institute for Space Research (INPE), [Available online at <http://mtc-m16d.sid.inpe.br/col/sid.inpe.br/mtc-m19/2012/08.02.02.42/doc/publicacao.pdf>], 2012.

Liu, H., Wang, C., Lee, S.-K., and Enfield, D.: Atlantic Warm Pool Variability in the CMIP5 Simulations, *Journal of Climate*, 26, 5315–5336, <https://doi.org/10.1175/JCLI-D-12-00556.1>, 2013.

Liu, Z., Vavrus, S., He, F., Wen, N., and Zhong, Y.: Rethinking Tropical Ocean Response to Global Warming: The Enhanced Equatorial 10 Warming*, *Journal of Climate*, 18, 4684–4700, <https://doi.org/10.1175/JCLI3579.1>, 2005.

Manabe, S. and Stouffer, R. J.: Sensitivity of a global climate model to an increase of CO₂ concentration in the atmosphere, *Journal of Geophysical Research*, 85, 5529–5554, <https://doi.org/10.1029/JC085iC10p05529>, 1980.

Manabe, S. and Wetherald, R. T.: Thermal Equilibrium of the Atmosphere with a Given Distribution of Relative Humidity, *Journal of the Atmospheric Sciences*, 24, 241–259, 1967.

15 Manabe, S. and Wetherald, R. T.: The Effects of Doubling the CO₂ Concentration on the climate of a General Circulation Model, *Journal of the Atmospheric Sciences*, 32, 3–15, [https://doi.org/10.1175/1520-0469\(1975\)032<0003:TEODTC>2.0.CO;2](https://doi.org/10.1175/1520-0469(1975)032<0003:TEODTC>2.0.CO;2), 1975.

Marengo, J. A. and Hastenrath, S.: Case Studies of Extreme Climatic Events in the Amazon Basin, *Journal of Climate*, 6, 617–627, [https://doi.org/10.1175/1520-0442\(1993\)006<0617:CSOECE>2.0.CO;2](https://doi.org/10.1175/1520-0442(1993)006<0617:CSOECE>2.0.CO;2), 1993.

Marvel, K. and Bonfils, C.: Identifying external influences on global precipitation, *Proceedings of the National Academy of Sciences*, 110, 20 19 301–19 306, <https://doi.org/10.1073/pnas.1314382110>, <http://www.pnas.org/cgi/doi/10.1073/pnas.1314382110>, 2013.

McCarthy, G. D., Smeed, D. A., Johns, W. E., Frajka-Williams, E., Moat, B. I., Rayner, D., Baringer, M. O., Meinen, C. S., Collins, J., and Bryden, H. L.: Measuring the Atlantic Meridional Overturning Circulation at 26° N, *Progress in Oceanography*, 130, 91–111, <https://doi.org/10.1016/j.pocean.2014.10.006>, 2015.

Mellor, G. L. and Yamada, T.: Development of a turbulence closure model for geophysical fluid problems, *Reviews of Geophysics*, 20, 851, 25 <https://doi.org/10.1029/RG020i004p00851>, 1982.

Miller, R. L., Schmidt, G. A., and Shindell, D. T.: Forced annular variations in the 20th century Intergovernmental Panel on Climate Change Fourth Assessment Report models, *Journal of Geophysical Research*, 111, <https://doi.org/10.1029/2005JD006323>, 2006.

Morrison, H., Curry, J. A., and Khvorostyanov, V. I.: A New Double-Moment Microphysics Parameterization for Application in Cloud and Climate Models. Part I: Description, *Journal of the Atmospheric Sciences*, 62, 1665–1677, <https://doi.org/10.1175/JAS3446.1>, 2005.

30 Nobre, P. and Shukla, J.: Variations of Sea Surface Temperature, Wind Stress, and Rainfall over the Tropical Atlantic and South America, *Journal of Climate*, 9, 2464–2479, [https://doi.org/10.1175/1520-0442\(1996\)009<2464:VOSSTW>2.0.CO;2](https://doi.org/10.1175/1520-0442(1996)009<2464:VOSSTW>2.0.CO;2), 1996.

Nobre, P., Siqueira, L. S. P., de Almeida, R. A. F., Malagutti, M., Giarolla, E., Castelão, G. P., Bottino, M. J., Kubota, P., Figueroa, S. N., Costa, M. C., Baptista, M., Irber, L., and Marcondes, G. G.: Climate Simulation and Change in the Brazilian Climate Model, *Journal of Climate*, 26, 6716–6732, <https://doi.org/10.1175/JCLI-D-12-00580.1>, 2013.

35 Park, S. and Bretherton, C. S.: The University of Washington Shallow Convection and Moist Turbulence Schemes and Their Impact on Climate Simulations with the Community Atmosphere Model, 22, 3449–3469, <https://doi.org/10.1175/2008JCLI2557.1>, <http://journals.ametsoc.org/doi/abs/10.1175/2008JCLI2557.1>, 2009.

Pincus, R., Forster, P. M., and Stevens, B.: The Radiative Forcing Model Intercomparison Project (RFMIP): experimental protocol for CMIP6, *Geoscientific Model Development*, 9, 3447–3460, <https://doi.org/10.5194/gmd-9-3447-2016>, 2016.

Pithan, F. and Mauritsen, T.: Arctic amplification dominated by temperature feedbacks in contemporary climate models, *Nature Geoscience*, 7, 181–184, <https://doi.org/10.1038/ngeo2071>, 2014.

5 Plass, G. N.: The Carbon Dioxide Theory of Climatic Change, *Tellus*, 8, 140–154, <https://doi.org/10.1111/j.2153-3490.1956.tb01206.x>, 1956.

Richter, I., Xie, S.-P., Behera, S. K., Doi, T., and Masumoto, Y.: Equatorial Atlantic variability and its relation to mean state biases in CMIP5, *Climate Dynamics*, 42, 171–188, <https://doi.org/10.1007/s00382-012-1624-5>, 2014.

Seager, R., Naik, N., and Vecchi, G. A.: Thermodynamic and Dynamic Mechanisms for Large-Scale Changes in the Hydrological Cycle in 10 Response to Global Warming*, *Journal of Climate*, 23, 4651–4668, <https://doi.org/10.1175/2010JCLI3655.1>, <http://journals.ametsoc.org/doi/abs/10.1175/2010JCLI3655.1>, 2010.

Shell, K. M., Kiehl, J. T., and Shields, C. a.: Using the radiative kernel technique to calculate climate feedbacks in NCAR's Community Atmospheric Model, *Journal of Climate*, 21, 2269–2282, <https://doi.org/10.1175/2007JCLI2044.1>, 2008.

Slingo, J. M.: The Development and Verification of A Cloud Prediction Scheme For the ECMWF Model, *Quarterly Journal of the Royal 15 Meteorological Society*, 113, 899–927, <https://doi.org/10.1002/qj.49711347710>, 1987.

Soden, B. and Held, I.: An Assessment of Climate Feedbacks in Coupled Ocean – Atmosphere Models, *Journal of Climate*, 19, 3354–3360, <https://doi.org/10.1175/JCLI9028.1>, 2006.

Soden, B. J., Broccoli, A. J., and Hemler, R. S.: On the use of cloud forcing to estimate cloud feedback, *Journal of Climate*, 17, 3661–3665, [https://doi.org/10.1175/1520-0442\(2004\)017<3661:OTUOCF>2.0.CO;2](https://doi.org/10.1175/1520-0442(2004)017<3661:OTUOCF>2.0.CO;2), 2004.

20 Soden, B. J., Held, I. M., Colman, R., Shell, K. M., Kiehl, J. T., and Shields, C. A.: Quantifying Climate Feedbacks Using Radiative Kernels, *Journal of Climate*, 21, 3504–3520, <https://doi.org/10.1175/2007JCLI2110.1>, 2008.

Soden, B. J., Collins, W. D., and Feldman, D. R.: Reducing uncertainties in climate models, *Science*, 361, 326–327, <https://doi.org/10.1126/science.aau1864>, <http://www.sciencemag.org/lookup/doi/10.1126/science.aau1864>, 2018.

Tarasova, T. a. and Fomin, B. a.: The Use of New Parameterizations for Gaseous Absorption in the CLIRAD-SW Solar Radiation Code for 25 Models, *Journal of Atmospheric and Oceanic Technology*, 24, 1157–1162, <https://doi.org/10.1175/JTECH2023.1>, 2007.

Taylor, K. E., Stouffer, R. J., and Meehl, G. a.: An overview of CMIP5 and the experiment design, *Bulletin of the American Meteorological Society*, 93, 485–498, <https://doi.org/10.1175/BAMS-D-11-00094.1>, 2012.

Tiedtke, M.: The sensitivity of the time mean large-scale flow to cumulus convection in the ECMWF model. Workshop on Convection in Large-Scale Numerical Model, pp. 297–316, ECMWF, 1984.

30 Veiga, S. F., Nobre, P., Giarolla, E., Capistrano, V., Baptista Jr., M., Marquez, A. L., Figueroa, S. N., Bonatti, J. P., Kubota, P., and Nobre, C. A.: The Brazilian Earth System Model version 2.5: Evaluation of its CMIP5 historical simulation, *Geoscientific Model Development Discussions*, pp. 1–73, <https://doi.org/10.5194/gmd-2018-91>, 2019a.

Veiga, S. F., Nobre, P., Giarolla, E., Capistrano, V., Baptista Jr., M., Marquez, A. L., Figueroa, S. N., Bonatti, J. P., Kubota, P., and Nobre, C. A.: The Brazilian Earth System Model ocean–atmosphere (BESM-OA) version 2.5: evaluation of its CMIP5 historical simulation, 12, 35 1613–1642, <https://doi.org/10.5194/gmd-12-1613-2019>, <https://www.geosci-model-dev.net/12/1613/2019/>, 2019b.

Vial, J., Dufresne, J.-L., and Bony, S.: On the interpretation of inter-model spread in CMIP5 climate sensitivity estimates, *Climate Dynamics*, 41, 3339–3362, <https://doi.org/10.1007/s00382-013-1725-9>, 2013.

Webster, S., Brown, A. R., Cameron, D. R., and P. Jones, C.: Improvements to the representation of orography in the Met Office Unified Model, 129, 1989–2010, <https://doi.org/10.1256/qj.02.133>, <http://doi.wiley.com/10.1256/qj.02.133>, 2003.

Xie, S.-P., Deser, C., Vecchi, G. A., Collins, M., Delworth, T. L., Hall, A., Hawkins, E., Johnson, N. C., Cassou, C., Giannini, A., and Watanabe, M.: Towards predictive understanding of regional climate change, *Nature Climate Change*, 5, 921–930, 5 <https://doi.org/10.1038/nclimate2689>, 2015.

Xue, Y., Sellers, P. J., Kinter, J. L., and Shukla, J.: A simplified biosphere model for global climate studies, *Journal of Climate*, 4, 345–364, 1991.

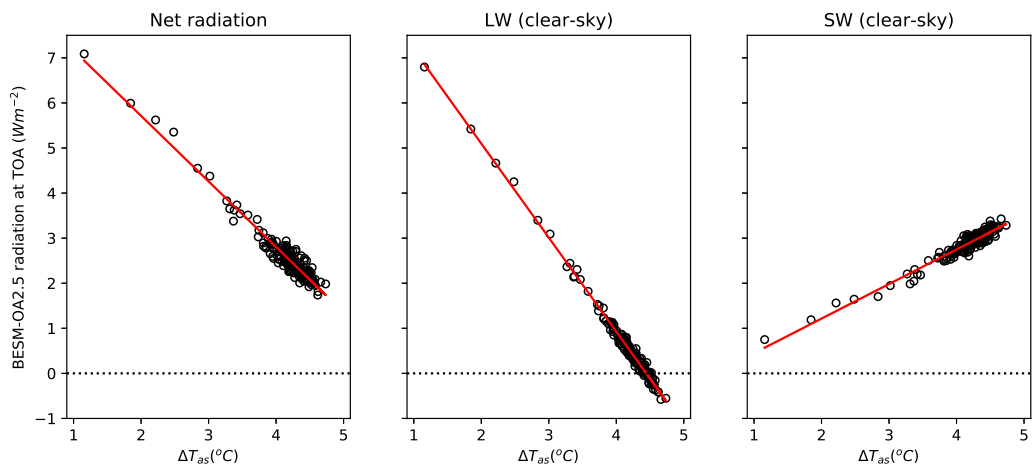


Figure 1. Annual global-mean linear regression between $\Delta\bar{T}_{as}$ and: (a) Net radiation, (b) ΔLW (clear-sky), and (c) ΔSW (clear-sky) for BESM-OA2.5

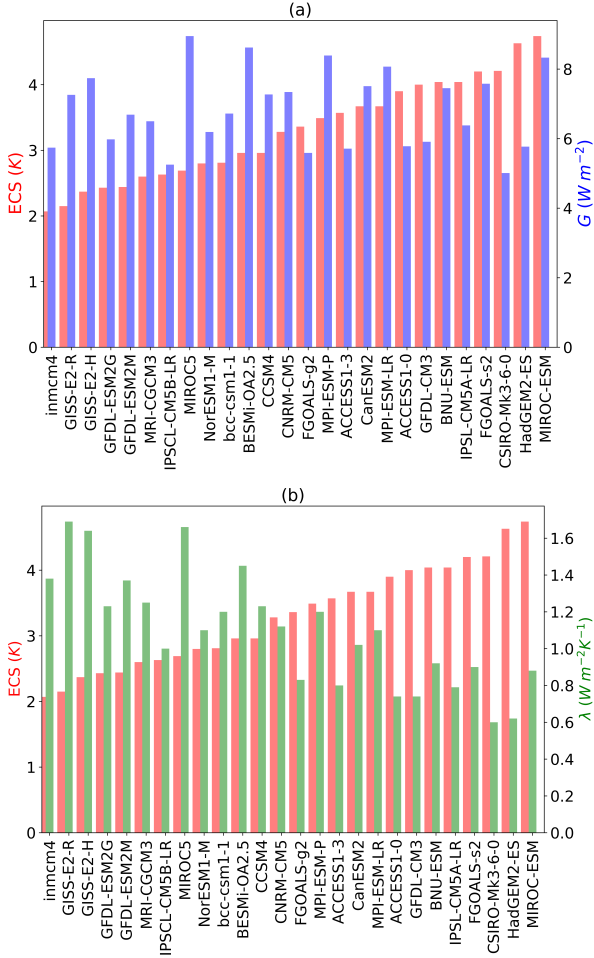


Figure 2. (a) Equilibrium Climate Sensitivity—climate sensitivity (ECS, in red) and Radiative forcing (G, in blue) values with ECS values increasing from left to right; (b) ECS (red) and climate sensitivity (λ , in green) with ECS values increasing from left to right.

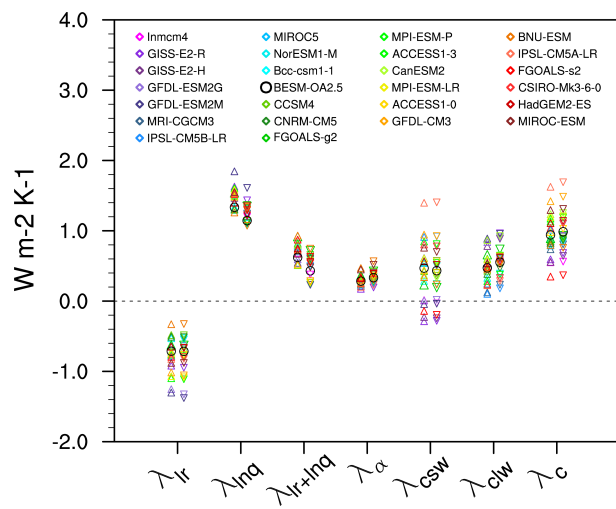


Figure 3. Global-mean feedbacks for 25 CMIP5 models and BESM-OA2.5 (circle). Changes in abrupt4xCO₂ relative to [the](#) piControl [are](#) [were](#) averaged over years [120-150](#). The triangles [represent the](#) mean estimated feedback values [calculated](#) using [the](#) NCAR radiative kernel whereas [the](#) upside-down triangles [mean represent the](#) estimated feedback values [calculated](#) using [the](#) GFDL radiative kernel.

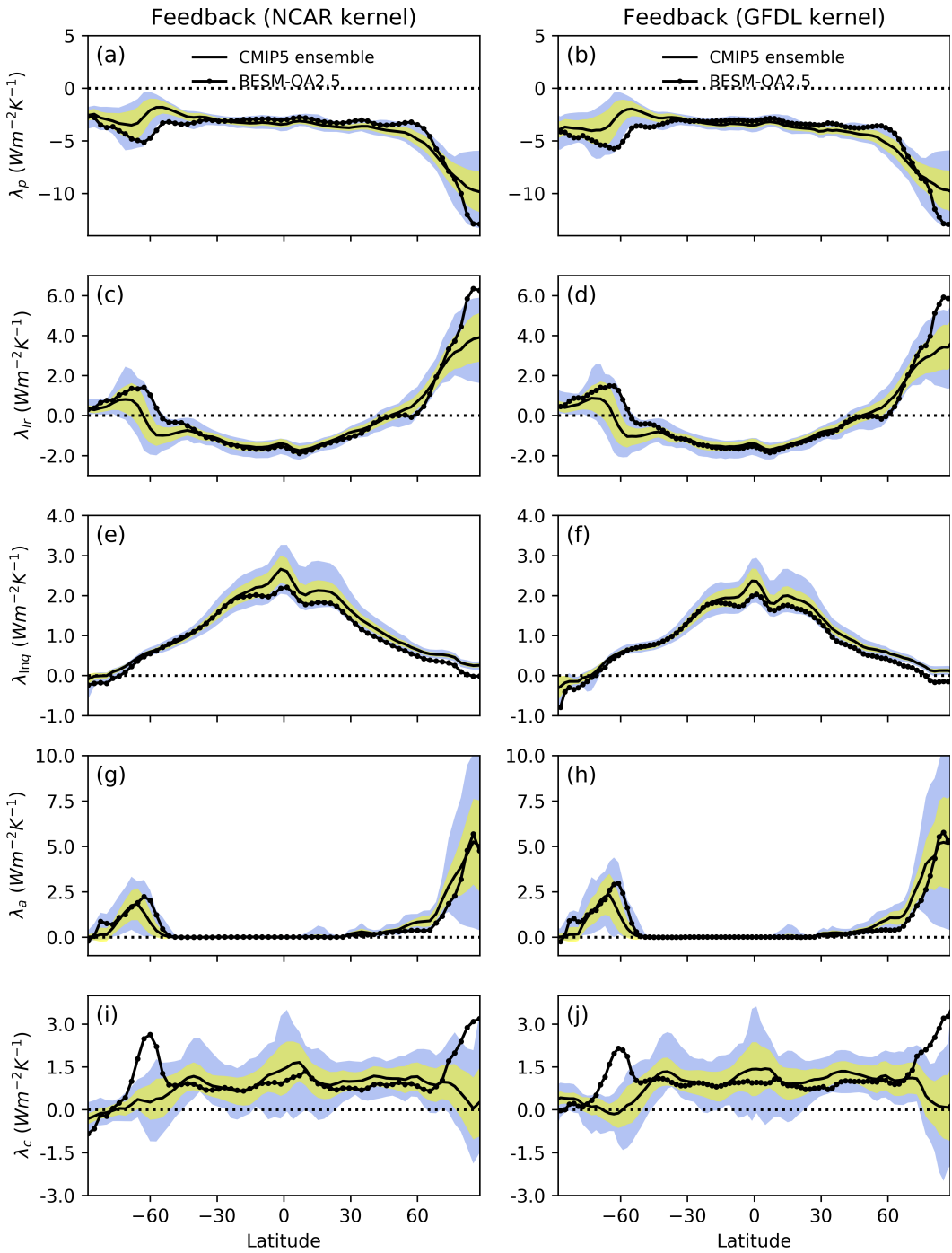


Figure 4. Feedbacks for the CMIP5 multi-model ensemble-mean (solid line) and BESM-OA2.5 (solid line with dots) for the Planck feedback (a and b), lapse-rate feedback (c and d), water vapor feedback (e and f), albedo feedback (g and h), and cloud feedback (i and j). Inter-model standard deviations for each latitude are in yellow. In blue are the feedback limits based on the maximum and minimum values for each latitude among the models, ~~not including~~ ~~excluding~~ BESM-OA2.5. All feedbacks are based on the averaged over years 120-150.

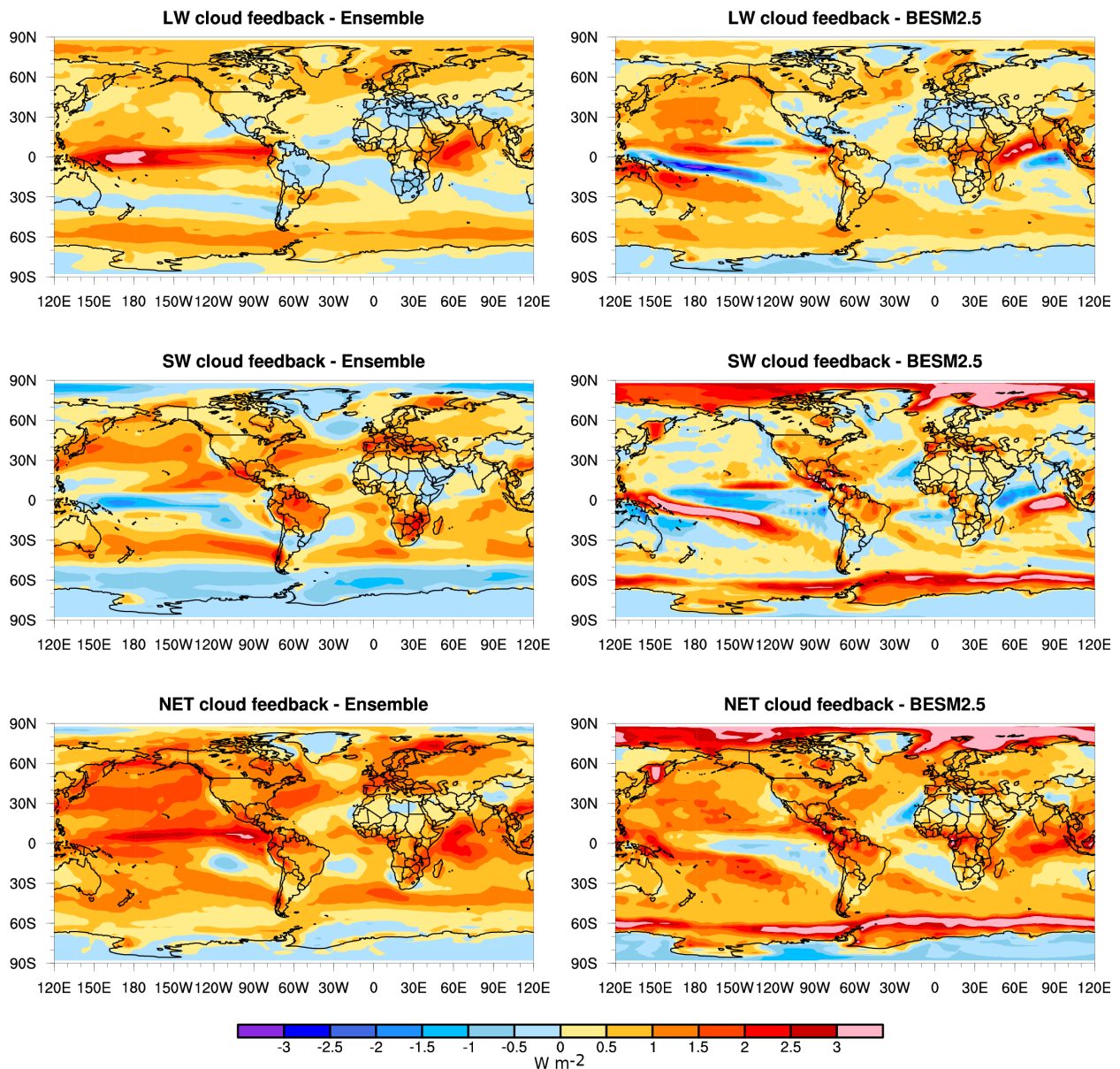


Figure 5. Cloud feedbacks [calculated](#) using the NCAR radiative kernel for [the](#) CMIP5 ensemble (left column) and BESM-OA2.5 (right column). [These](#) [These](#) results are based on the averaged [over](#) [from](#) years [120-150](#); [120-150](#).

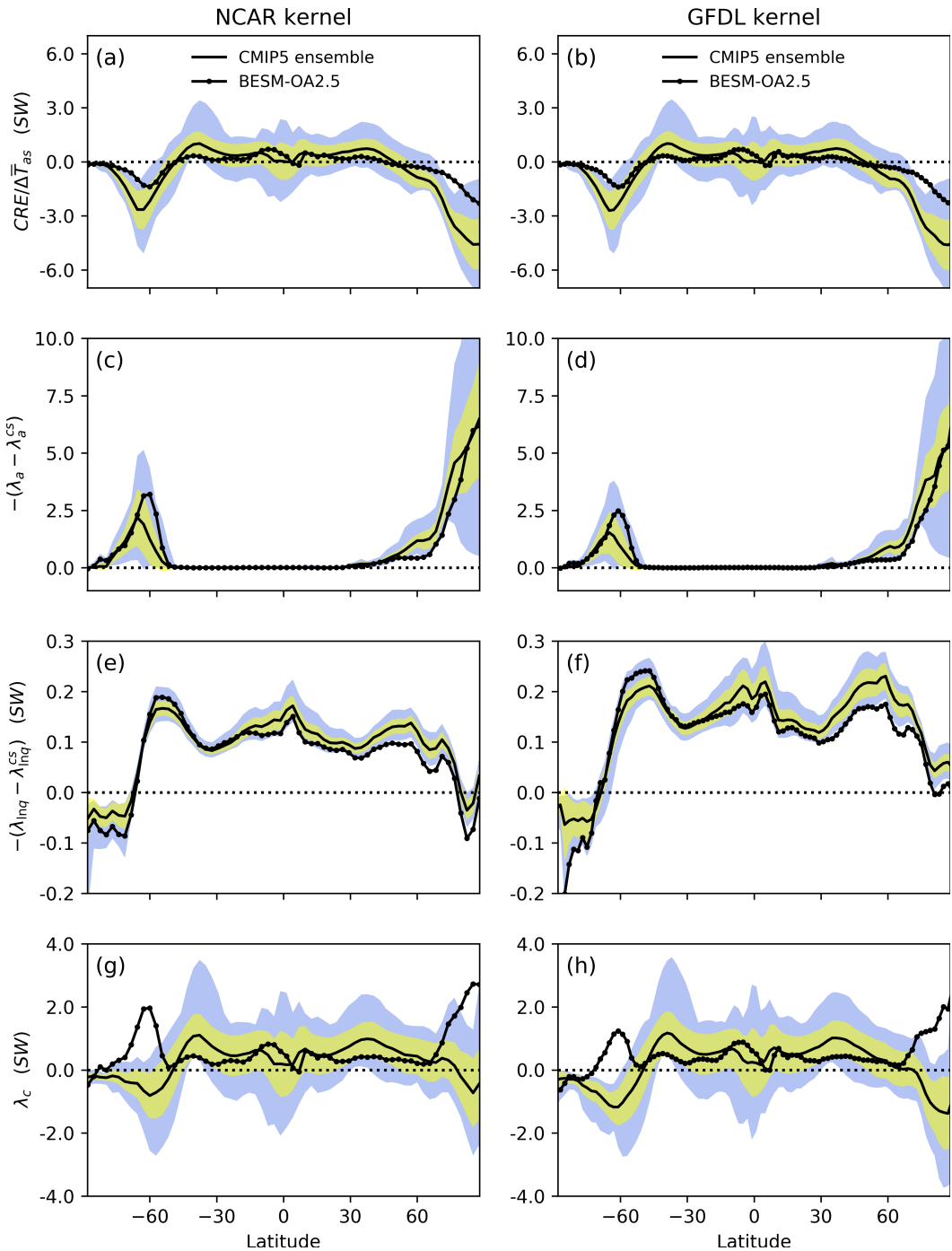


Figure 6. SW-Cloud feedback. Shortwave cloud radiative effect (a and b), the albedo (c and d), SW humidity (e and f), feedbacks cloud masking, and shortwave cloud feedback (g and h) for the CMIP5 multi-model ensemble-mean (solid line) and BESM-OA2.5 (solid line with dots). Inter-model standard deviations for each latitude are in yellow. In blue are the feedback limits based on the maximum and minimum values for each latitude among the models, ~~not including~~ excluding BESM-OA2.5.

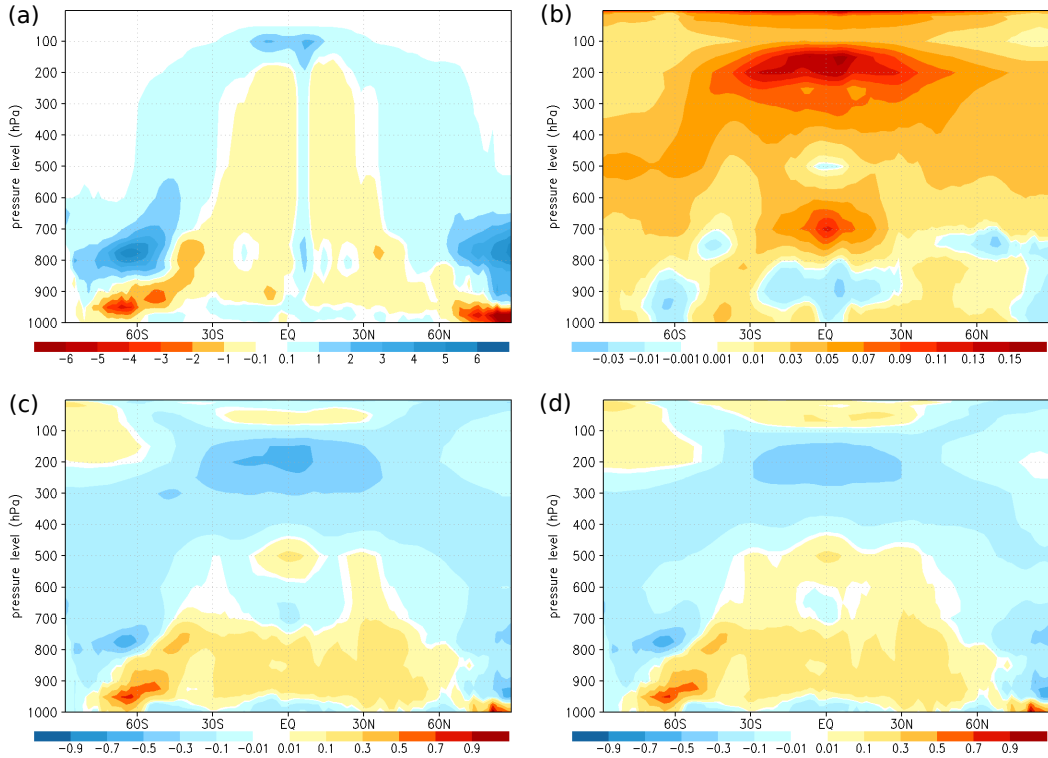


Figure 7. Vertical profiles of the zonal mean of the $4\times\text{CO}_2$ - $4\times\text{CH}_4$ - piControl mean difference for the following variables: (a) Cloud fraction, (b) shortwave, (c) long wave and (d) sum of the shortwave and longwave for BESM-OA2.5.

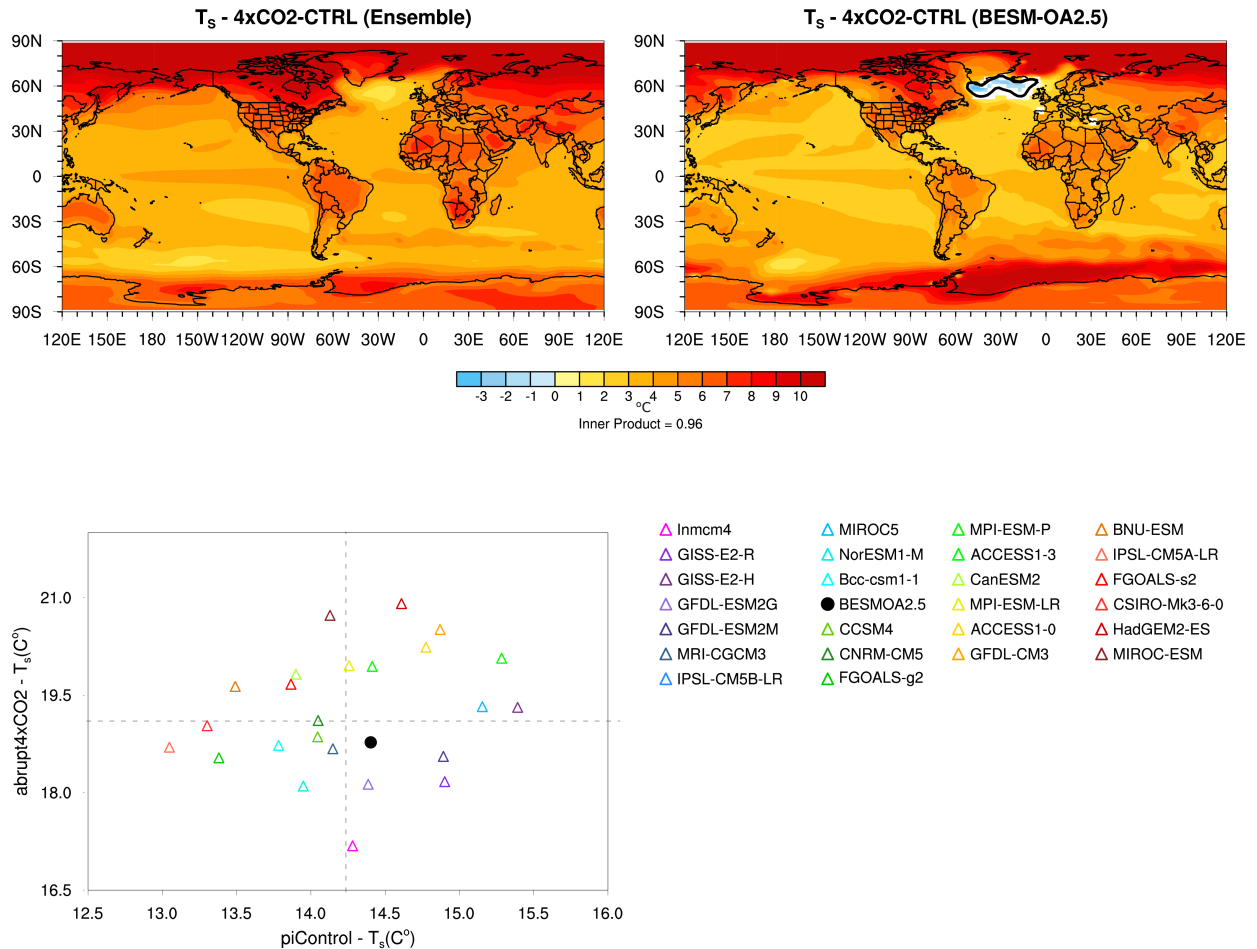


Figure 8. Difference **Differences** (averaged over years 120–150) **of** **in** **surface temperature** **between** **the** **abrupt4xCO2** **and** **piControl** **simulations** **in** **(a)** **the** **CMIP5** **ensemble** **and** **(b)** **in** **BESM-OA2.5**; **and** **(c)** **A** **scatter** **plot** **of** **the** **global** **average** **of** **surface temperature** **for** **the** **CMIP5** **models** **used** **in** **the** **ensemble** **and** **BESM-OA2.5** (black dot). **Shaded** **The shaded** **areas** **in** **(a)** **and** **(b)** **have** **level** **of** **confidence** **level** **greater** **than** **90%**; **the** **black** **line** **represents** **the** **isoline** **of** **zero** **temperature** **difference**.

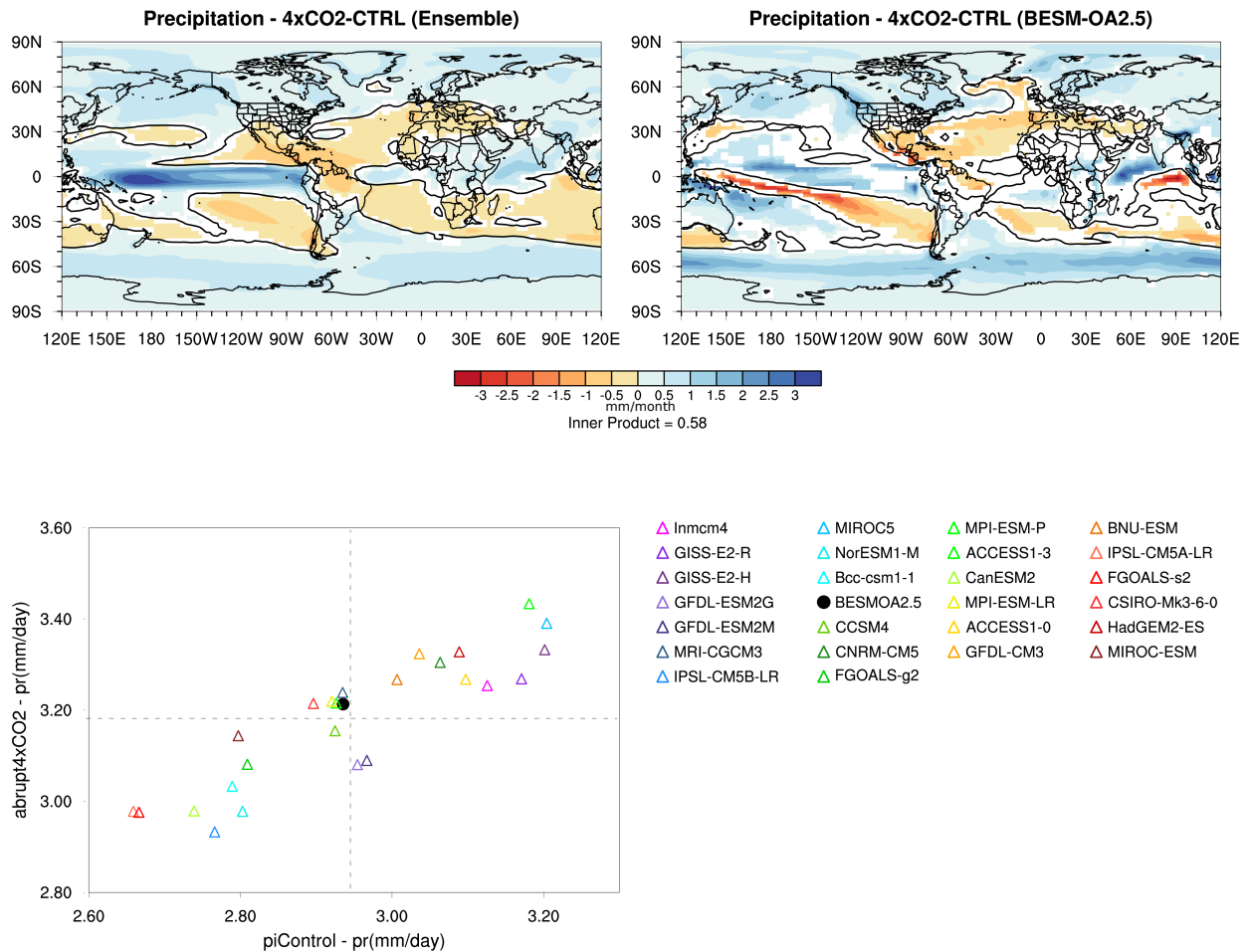


Figure 9. Difference-Differences (averaged over years 120-150) of in precipitation (in mm/month) between the abrupt4xCO2 and the piControl simulations in (a) CMIP5 ensemble and (b) in BESM-OA2.5 -(c) A scatter plot of the precipitation global average averages for the CMIP5 models used in the ensemble and BESM-OA2.5 (black dot). Shaded-The shaded areas in (a) and (b) have level of confidence levels greater than 90%; the black line represents the isoline of zero precipitation difference.

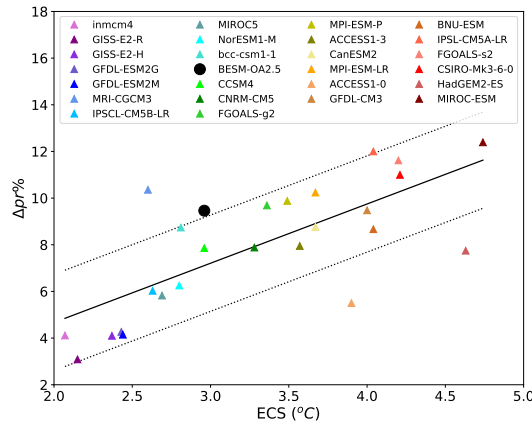


Figure 10. Scatter plot between of the ECS and $\Delta\text{Pr}\%$ values for all of the ensemble models considered. The solid black line is shows the linear fit between the ECS and the perceptual change in precipitation change. As in Figure 2, the models are sorted according their ECS value. The dash lines represent the error limits considering the residual standard error.

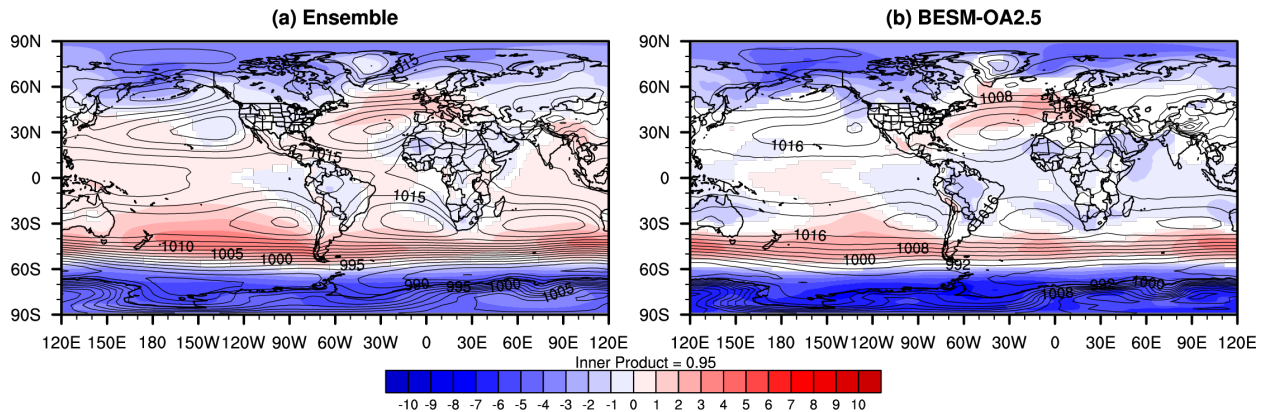


Figure 11. Difference (averaged over years 120-150) of in sea level pressure (SLP) in hPa between two scenarios (abrupt4xCO₂ minus piControl, shaded), and SLP during under piControl conditions (contours) in CMIP5 models ensemble (first column) and BESM-OA2.5 (second column). The white areas have level of confidence levels less than 90%.

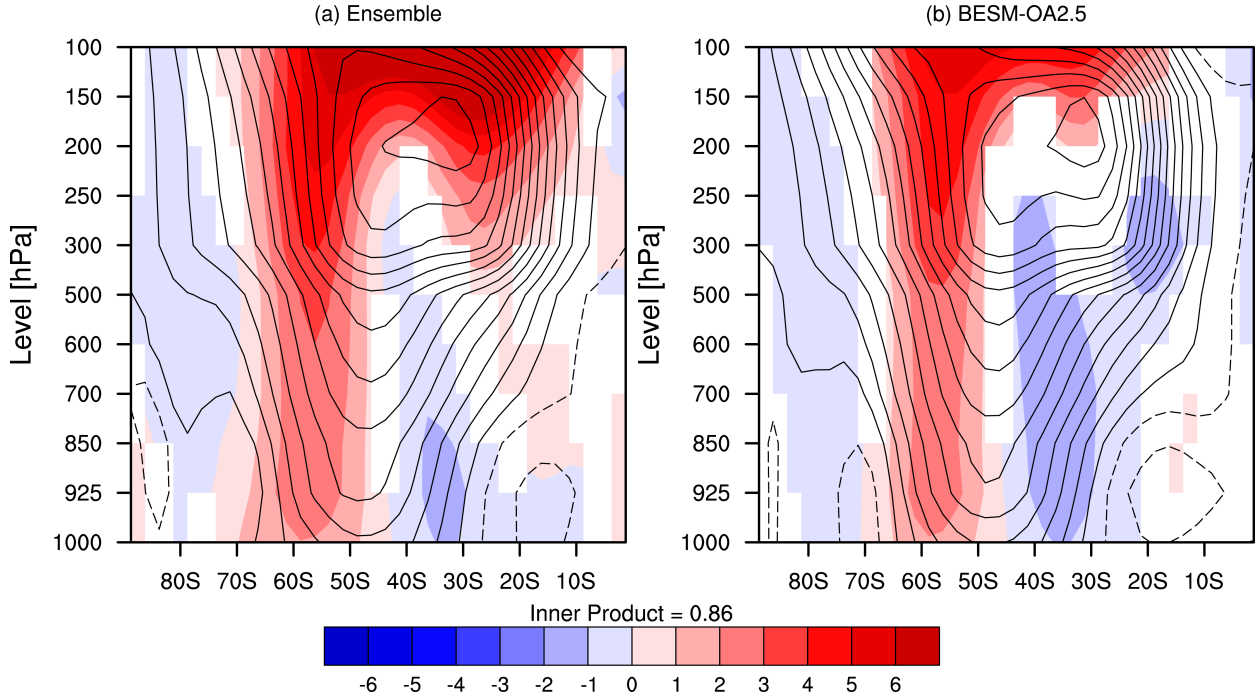


Figure 12. Vertical profile of the difference (averaged over years 120-150) of in the zonal mean wind (in m/s) between two scenarios (abrupt4xCO2 minus piControl, shaded), and the piControl conditions (contours) for (a) the ensemble of CMIP5 models and for (b) BESM-OA2.5. White regions have level of confidence levels less than 90%.

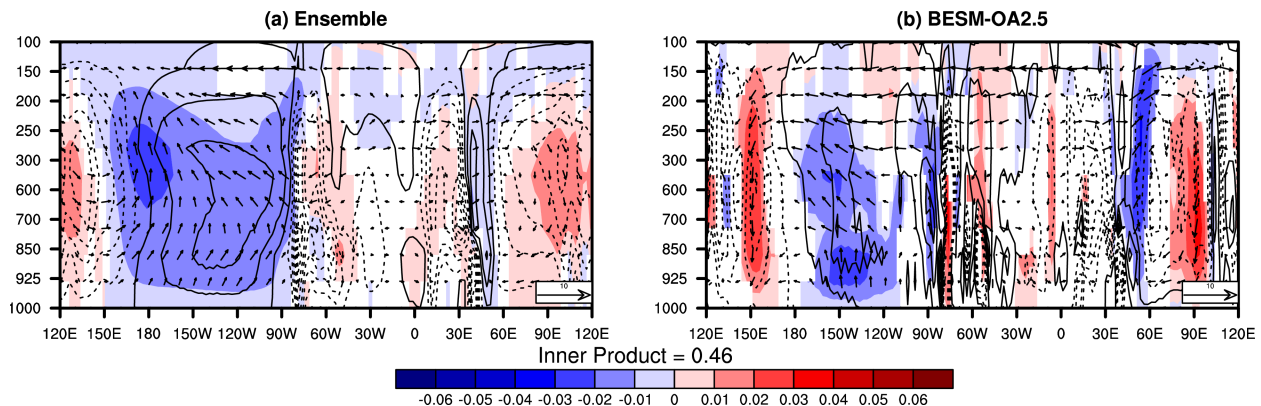


Figure 13. Difference (averaged over years 120-150) between the abrupt4xCO2 and piControl conditions for omega (shades) in Pa/s and zonal vertical winds (vectors), averaged between 5°S and 5°N, for (a) the CMIP5 ensemble and (b) BESM-OA2.5. Contours represent the averaged piControl omega in the same region. White areas have a level of confidence levels less than 90%.

Table 1. Atmospheric physical parameterizations used in BAM (Figueroa et al., 2016) BESM-OA2.5.

Physical Parameterization	BAM	BESM-OA2.5
Shortwave radiation	RRTMG (Iacono et al., 2008)	Clirad (Tarasova and Fomin, 2007)
Longwave radiation	RRTMG (Iacono et al., 2008)	Harshvardhan et al. (1987)
Cloud microphysics	Morrison (Morrison et al., 2005)	Ferrier et al. (2002)
Land surface model	Ibis [Foley et al. (1996) modified by Kubota (2012)]	SSib (Xue et al., 1991)
Planetary Boundary Layer	Modified Mellor and Yamada (1982) scheme	Holtslag and Boville (1993) scheme
Shallow Convection	UW shallow convection (Park and Bretherton, 2009)	Tiedtke (1984)
Deep Convection	Modified Grell and Dévényi (2002) ensemble scheme	Modified Grell and Dévényi (2002) ensemble scheme
Gravity wave	Webster et al. (2003) scheme with low-level blocking	Alpert et al. (1988)
Total Cloud cover fraction	Based on Probability Density Function (PDF)	Slingo (1987)

Table 2. Models belonging to the CMIP5 ensemble used in this study.

Number	Model	Institution, country
1	ACCESS1-0	CSIRO-BOM, Australia
2	ACCESS1-3	
3	bcc-csm1-1	BCC, China
4	BNU-ESM	BNU, China
5	CanESM2	CCCma, Canada
6	CCSM4	NCAR, USA
7	CNRM-CM5	CNRM-CERFACS, France
8	CSIRO-Mk3-6-0	CSIRO-QCCCE, Australia
9	FGOALS-g2	LASG-CESS, China
10	FGOALS-s2	LASG-IAP, China
11	GFDL-CM3	
12	GFDL-ESM2G	NOAA-GFDL, USA
13	GFDL-ESM2M	
14	GISS-E2-H	NASA-GISS, USA
15	GISS-E2-R	
16	HadGEM2-ES	MOHC, England
17	inmcm4	INM, Russia
18	IPSL-CM5A-LR	IPSL, France
19	IPSL-CM5B-LR	
20	MIROC-ESM	
21	MIROC5	MIROC, Japan
22	MPI-ESM-LR	
23	MPI-ESM-P	MPI-M, Germany
24	MRI-CGCM3	MRI, Japan
25	NorESM1-M	NCC, Norway

Table 3. CO_2 - CO_2 Forcing (W m^{-2}) (G), Net Feedback ($\text{W m}^{-2} \text{K}^{-1}$) (λ), Climate Response ($\text{W m}^{-2} \text{K}^{-1}$) (ΔCRE), and Equilibrium climate sensitivity (K) (ECS) values.

Model	G	λ	ΔCRE	ECS
ACCESS1-0	5.78	-0.74	0.11	3.90
ACCESS1-3	5.71	-0.80	0.27	3.57
bcc-csm1-1	6.72	-1.20	-0.06	2.81
BESM-OA2.5	8.62	-1.45	-0.13	2.96
BNU-ESM	7.45	-0.92	-0.27	4.04
CanESM2	7.51	-1.02	0.16	3.67
CCSM4	7.27	-1.23	-0.15	2.96
CNRM-CM5	7.34	-1.12	-0.19	3.28
CSIRO-Mk3-6-0	5.01	-0.60	0.25	4.21
FGOALS-g2	5.59	-0.83	-0.08	3.36
FGOALS-s2	7.58	-0.90	-0.45	4.20
GFDL-CM3	5.91	-0.74	0.49	4.00
GFDL-ESM2G	5.98	-1.23	-0.21	2.43
GFDL-ESM2M	6.69	-1.37	-0.31	2.44
GISS-E2-H	7.74	-1.64	-0.50	2.37
GISS-E2-R	7.26	-1.69	-0.46	2.15
HadGEM2-ES	5.77	-0.62	0.37	4.63
inmcm4	5.74	-1.38	-0.10	2.07
IPSL-CM5A-LR	6.38	-0.79	0.70	4.04
IPSL-CM5B-LR	5.25	-1.00	0.29	2.63
MIROC5	8.95	-1.66	-0.43	2.69
MIROC-ESM	8.33	-0.88	0.14	4.74
MPI-ESM-LR	8.07	-1.10	-0.06	3.67
MPI-ESM-P	8.39	-1.20	-0.04	3.49
MRI-CGCM3	6.50	-1.25	-0.05	2.60
NorESM1-M	6.19	-1.10	-0.08	2.80
Mean	6.84 ± 1.09	-1.09 ± 0.31	-0.03 ± 0.30	3.30 ± 0.76